OAK RIDGE NATIONAL LABORATORY LIBRARIES
3 4456 0549122 3

CENTRAL RESEARCH LIBRARY
DOCUMENT COLLECTION

35

ONAL LABORATORY
operated by
UNION CARBIDE CORPORATION
for the
U. S. ATOMIC ENERGY COMMISSION

UNION CARBIDE

ORNL-TM-534

CONDENSING FLOW IN FINNED, TAPERED TUBES

R. B. Korsmeyer

CENTRAL RESEARCH LIBRARY
DOCUMENT COLLECTION
LIBRARY LOAN COPY
DO NOT TRANSFER TO ANOTHER PERSON
If you wish someone else to see this document, send in name with document and the library will arrange a loan.

NOTICE

This document contains information of a preliminary nature and was prepared primarily for internal use at the Oak Ridge National Laboratory. It is subject to revision or correction and therefore does not represent a final report. The information is not to be abstracted, reprinted or otherwise given public dissemination without the approval of the ORNL patent branch, Legal and Information Control Department.

LEGAL NOTICE

This report was prepared as an account of Government sponsored work. Neither the United States, nor the Commission, nor any person acting on behalf of the Commission:

A. Makes any warranty or representation, expressed or implied, with respect to the accuracy, completeness, or usefulness of the information contained in this report, or that the use of any information, apparatus, method, or process disclosed in this report may not infringe privately owned rights; or

B. Assumes any liabilities with respect to the use of, or for damages resulting from the use of any information, apparatus, method, or process disclosed in this report.

As used in the above, "person acting on behalf of the Commission" includes any employee or contractor of the Commission, or employee of such contractor, to the extent that such employee or contractor of the Commission, or employee of such contractor prepares, disseminates, or provides access to, any information pursuant to his employment or contract with the Commission, or his employment with such contractor.

ORNL-TM-534

Contract No. W-7405-eng-26

Reactor Division

CONDENSING FLOW IN FINNED, TAPERED TUBES

R. B. Korsmeyer

Date Issued

MAY - 1 1963

OAK RIDGE NATIONAL LABORATORY
Oak Ridge, Tennessee
operated by
UNION CARBIDE CORPORATION
for the
U.S. ATOMIC ENERGY COMMISSION

OAK RIDGE NATIONAL LABORATORY LIBRARIES

3 4456 0549122 3

CONTENTS

Abstract v
Basic Conditions 2
Geometrical Considerations 2
Heat Transfer and Tube Length 3
Friction Pressure Drop 7
Momentum Pressure Recovery 14
Over-All Condensing Pressure Drop 23
Parallel Flow Stability 23
Table of Nomenclature 37
Notes 39
References 40

Abstract

On the assumption that a Lockhart-Martinelli type of correlation is applicable, an analytical approach to the interpretation of pressure drop data on condensing flow in tapered tubes is developed with particular reference to the condensation of potassium in a radiant condenser of a type that may be attractive for space power plants. It appears that instability can be encountered in such condensers only through the introduction of excess liquid inventory at reduced power or by design of the condenser for insufficient pressure drop at design power.

Condensing Flow in Finned, Tapered Tubes

The purpose of this study is the development of an analytical approach to the interpretation of experimental data on the two-phase pressure drop characteristic of condensing flow in the tapered tubes of a radiant condenser. The study is particularly concerned with the behavior of condensing potassium at rather low pressure (1.5 psia), and it assumes that a Lockhart-Martinelli type of correlation is applicable — an assumption that must be established experimentally.

The Lockhart-Martinelli[1] correlation of two-phase, two-component flow utilizes the ratio of the actual pressure gradient to the pressure gradient of the gas phase flowing alone (virtual gas pressure gradient) as an empirically determined function of a two-phase flow modulus which, in turn, is a function of the virtual liquid and gas pressure gradient ratios. The mathematical form is as follows:

$$\phi^2 = \frac{\left(\frac{\Delta P}{\Delta z}\right)_{TP}}{\left(\frac{\Delta P}{\Delta z}\right)_g} \tag{1}$$

$$X^2 = \frac{\left(\frac{\Delta P}{\Delta z}\right)_\ell}{\left(\frac{\Delta P}{\Delta z}\right)_g} \tag{2}$$

and

$$\phi^2 = f\,(X) \tag{3}$$

Since $(\Delta P/\Delta z)_g$ can be calculated from the Fanning friction factor for the pertinent flow conditions, the actual, two-phase pressure drop can be determined from an empirical correlation of ϕ^2 with X.

This treatment has been applied to condensing mercury flow in cylindrical tubes by Baroczy and Sanders[2] by means of an empirical correlation of ϕ^2 vs X for noncondensing flow of mercury and nitrogen. An improvement was obtained in the correlation by including the gas phase turbulent Reynolds number as an empirical variable. In other words, ϕ^2 is a function of both X and N_{Rg}:

$$\phi^2 = f\,(X_{vt},\ N_{R_g}) \tag{4}$$

The present study is an extension of the Baroczy and Sanders treatment to the condensing flow of potassium in finned, tapered tubes that appear to be attractive for heat sinks in satellite power plants.

Basic Conditions

Throughout the study it is assumed that the physical properties of both liquid and vapor remain constant, except for the vapor density. It is further assumed that the temperature of the radiative surface is constant over the condensing portion of the tube, which is not strictly true as the tube surface is necessarily hotter than the tips of the fins. However, the fin efficiency is factored into the equations via a reduction in the value of the actual external surface to an "effective" heat transfer surface at which the heat flux is considered constant.

The temperature drop from the condensing vapor to the radiating surface is considered negligible, except as it is factored into the fin efficiency term.

Geometrical Considerations

Since the volume reduction on condensation is several orders of magnitude, a saving in structural weight can be obtained by the use of tapered condenser tubes,[3] and a prime consideration is the maximum acceptable vapor entrance velocity. If the vapor is of fairly high quality, the entrance losses at a properly faired tee connecting the tube to the manifold are very small for velocities as high as Mach 0.25, and the total condensing pressure drop through the tube will be in the neighborhood of 20% of the inlet pressure for good design. Increasing the entrance Mach number significantly beyond 0.25 results in a very rapid rise in condensing pressure drop and consequent extreme decrease of absolute pressure on the liquid leaving the condenser. For this reason, the entrance velocity was fixed at Mach 0.25 for the cases considered.

The inlet diameter is fixed by the condensing pressure, the entrance Mach number, and the weight flow desired. For a known radiative heat flux, coolant flow, and condensing pressure the tube length is fixed for a given fin size, and the entire tube geometry is thus determined.

Three cases for condensing potassium at 1500°R (1.5 psia) are considered in this study, in which fin height and tube diameter are the independently varied parameters. For liquid exit velocities of the order of 1 ft/sec a diameter reduction factor, D_o/D_L, of 4 was chosen. Since the tube length is determined by heat transfer considerations, the tube taper differs in each case.

As shown in Fig. 1, the tube wall was arbitrarily fixed at 0.050 in. and the fin thickness at 0.010 in. No attempt has been made to optimize either the tube wall or fin thickness.

Heat Transfer and Tube Length

For a space temperature approaching zero, the radiative heat flux is:

$$\frac{Q}{A_h} = \gamma \epsilon \sigma T_r^4 \tag{5}$$

where γ represents the view factor. The view factor depends, of course, on the tube diameter and spacing. However, it normally will lie between values of 0.8 and 0.9 for the model shown in Fig. 1.

The fin efficiency for rectangular fins is:[4]

$$\xi = \frac{\tanh y \sqrt{\frac{2 h_e}{kb}}}{y \sqrt{\frac{2 h_e}{kb}}} \tag{6}$$

For radiative heat transfer a fictitious coefficient is determined from the heat flux and fin absolute temperature:

$$h_e = \frac{Q}{A_h} \frac{1}{T_r} \tag{7}$$

If a copper fin thinly clad with, say, oxidized aluminum bronze is used, the efficiency becomes:

$$\xi = \frac{\tanh 6.91y}{6.91y} \tag{8}$$

for a view factor of 0.8, an emissivity of 0.86, and a radiating temperature of 1500°R.

Unclassified
ORNL-LR-DWG-79086

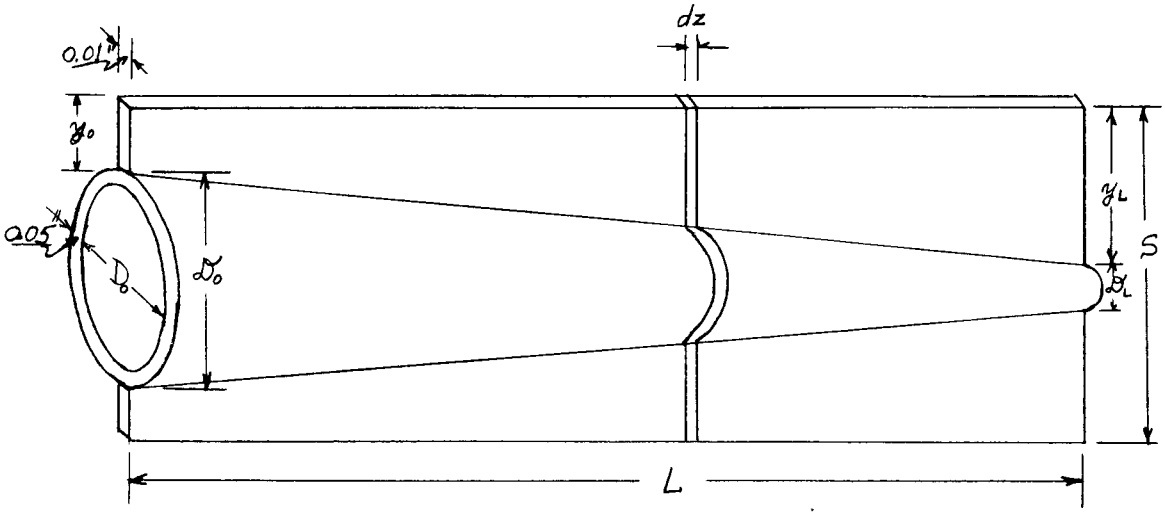

Fig. 1. Model Used for Heat Transfer and Fluid Flow Calculations.

For any given entrance fin height, y_o, the reduction in fin efficiency that occurs as y increases along the length of the tube to y_L can be considered linear. The efficiency at any point z therefore becomes:

$$\xi_z = \xi_o (1 - \eta\kappa) \tag{9}$$

The tube outside diameter also varies linearly with z and can be expressed as:

$$\mathcal{D}_z = \mathcal{D}_o (1 - \beta \kappa) \tag{10}$$

The fin span, s, is constant and equal to $(\mathcal{D}_o + 2 y_o)$. From Fig. 1 the differential effective heat transfer surface is:

$$dA_{hz} = [2 (s - \mathcal{D}_z) \xi_z + \pi D_z] dz \tag{11}$$

Substituting Eqs. 9 and 10 into Eq. 11 yields:

$$\frac{dA_{hz}}{dz} = 2\xi_o (1 - \eta\kappa) [s - \mathcal{D}_o (1 - \beta\kappa)] + \pi\mathcal{D}_o (1 - \beta\kappa) \tag{12}$$

or

$$\frac{dA_{hz}}{dz} = [4\xi_o y_o + \pi\mathcal{D}_o] + [2\xi_o\mathcal{D}_o\beta - 4\xi_o y_o\eta - \pi\mathcal{D}_o\beta]\kappa - [2\xi_o\mathcal{D}_o\eta\beta] \kappa^2 \tag{13}$$

$$A_{hz} = L\left[(4\xi_o y_o + \pi\mathcal{D}_o)\kappa + \left(\xi_o\mathcal{D}_o\beta - 2\xi_o y_o\eta - \frac{\pi}{2}\mathcal{D}_o\beta\right) \kappa^2 - \frac{2}{3} \xi_o\mathcal{D}_o\eta\beta\kappa^3\right] \tag{14}$$

since

$$dz = L \, d\kappa$$

The heat radiated by the entire tube is related to the heat transfer surface through Eq. 5:

$$Q_T = \gamma \epsilon \sigma T^4 A_{hL} \tag{15}$$

and A_{hL} is the value of A_{hz} when $\kappa = 1$:

$$A_{hL} = L\left[2\xi_o y_o (2 - \eta) + \pi\mathcal{D}_o \left(1 - \frac{\beta}{2}\right) + \mathcal{D}_o\xi_o\beta \left(1 - \frac{2}{3} \eta\right)\right] \tag{16}$$

The minimum tube length is determined by the limiting inlet vapor velocity for a given fluid and condensing pressure. The inlet vapor weight flow in terms involving the vapor velocity is:

$$W_{go} = v_{go} (3600) \rho_g A_o$$

$$W_{g_o} = 2820\, D_o^{\,2}\, \rho_g\, v_{g_o} \tag{17}$$

and the heat flow is:

$$Q = H\, W_{g_o} \tag{18}$$

From Eqs. 15 through 18 the tube length can be expressed as:

$$L = \frac{H\, W_{g_o}}{\gamma \epsilon \sigma T^4 \left[2\xi_o y_o\, (2 - \eta) + \pi \theta_o \left(1 - \frac{\beta}{2}\right) + \theta_o \xi_o \beta \left(1 - \frac{2}{3}\eta\right)\right]} \tag{19}$$

The sonic velocity in potassium vapor at 1500°R is about 1600 ft/sec, so that Eq. 19 takes the following form:

$$L_{M=0.25} = \frac{574\, D_o^{\,2}}{\left[2\xi_o y_o\, (2 - \eta) + \pi \theta_o \left(1 - \frac{\beta}{2}\right) + \theta_o \xi_o \beta \left(1 - \frac{2}{3}\eta\right)\right]} \tag{20}$$

From Eq. 20 the tube lengths were calculated for the following three cases:

Case	I	II	III
Po, psia	1.5	1.5	1.5
β	0.643	0.643	0.682
θ_o, in.	0.700	0.700	1.100
θ_L, in.	0.250	0.250	0.350
D_o, in.	0.600	0.600	1.000
D_L, in.	0.150	0.150	0.250
y_o, in.	0.600	0	1.000
y_L, in.	0.825	0.225	1.375
α	0.750	0.750	0.750
ξ_o	0.96	1.00	0.90
η	0.031	0	0.067
W_{g_o}, lb/hr	9.64	9.64	26.8
L, ft	4.10	8.85	7.44

Cases I and II show the effect of fin height on tube length; Cases II and III show the improvement in condensing capacity obtained by increasing both inlet diameter and fin height for nearly the same tube length.

Friction Pressure Drop

For condensation the ratio of liquid to vapor flow rates is:

$$\frac{W_\ell}{W_g} = \frac{W_\ell + W_c}{W_{g_o} - W_c} = \frac{W_T - W_{g_o} + W_c}{W_{g_o} - W_c} \quad \text{(Ref. 2)}$$

However,

$$\frac{W_c}{W_{g_o}} = \frac{A_{hz}}{A_{hL}},$$

and so,

$$\frac{W_\ell}{W_g} = \frac{1}{x_o\left(1 - \frac{A_{hz}}{A_{hL}}\right)} - 1 \tag{21}$$

The virtual gas mass velocity (i.e., the velocity of the gas phase flowing alone) is:

$$G_g = \frac{W_{g_o}}{A_z}\left(1 - \frac{A_{hz}}{A_{hL}}\right) \tag{22}$$

The average normalized heat transfer surface, A_{hz}/A_{hL}, is shown plotted against the normalized tube length, κ, in Fig. 2 for the three cases. The individual curves for the three cases differ negligibly, so that only a single relation is used in which the κ^3 term is neglected. The equation is:

$$\frac{A_{hz}}{A_{hL}} = 1.11\,\kappa - 0.10\,\kappa^2 \tag{23}$$

Substitution of Eq. 23 in Eq. 21 yields:

$$\frac{W_L}{W_g} = \left[\frac{1}{x_o\,(1 - 1.11\,\kappa + 0.10\,\kappa^2)} - 1\right] \tag{24}$$

Since

$$A_z = \frac{\pi}{4} D_z^{\,2} = \frac{\pi}{4} D_o^{\,2}\,(1 - \alpha\kappa)^2 \tag{25}$$

the gas mass velocity divided by the inlet weight flow is:

$$\frac{G_g}{W_{g_o}} = \frac{4}{\pi\,D_o^{\,2}\,(1 - \alpha\kappa)^2}\,[1 - 1.11\,\kappa + 0.10\,\kappa^2] \tag{26}$$

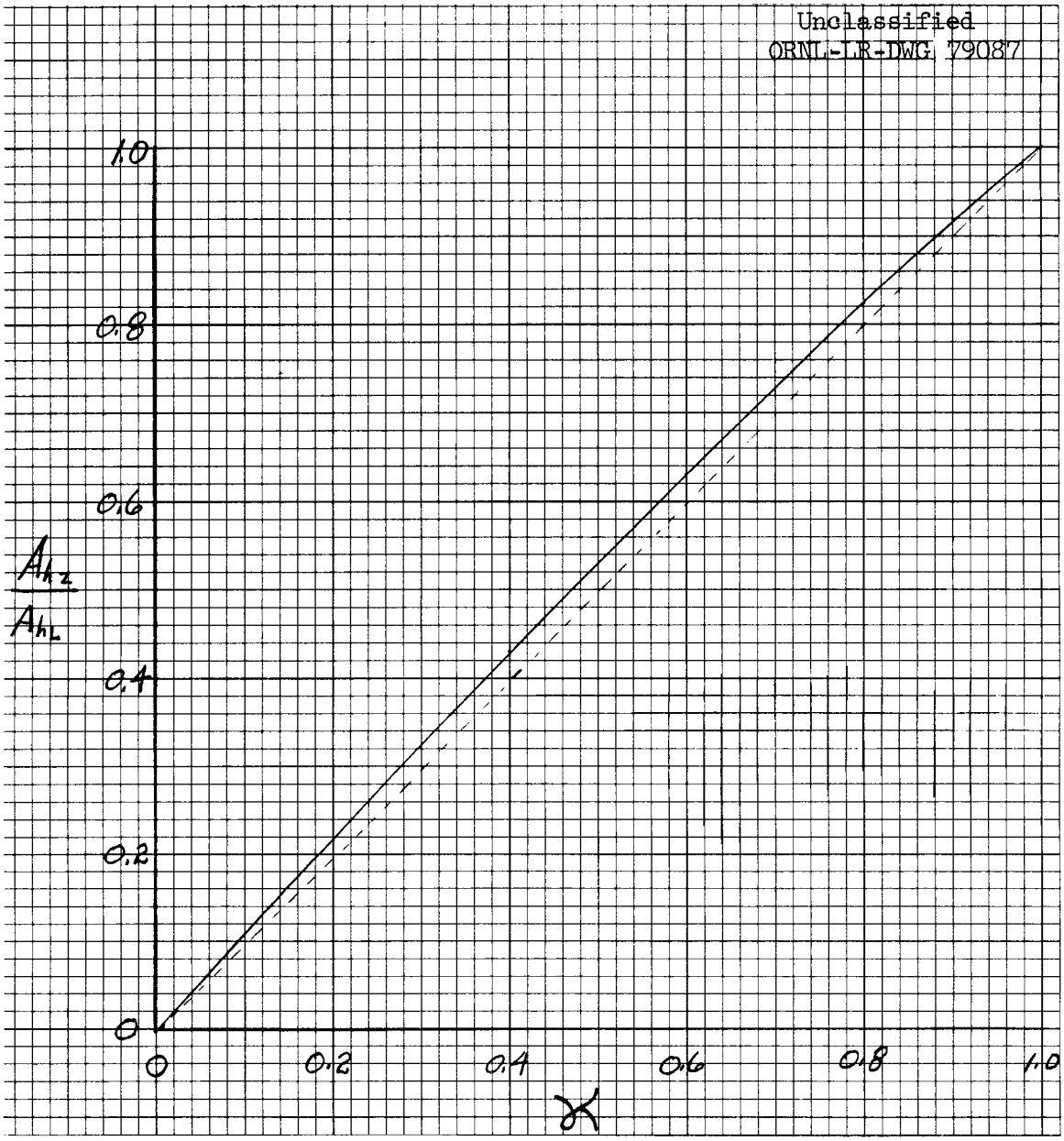

Fig. 2. Normalized Effective External Heat Transfer vs Normalized Tube Length.

Equations 24 and 26 are plotted in Fig. 3 for the three cases. The square root of W_ℓ/W_g is given, as this quantity is more useful in subsequent calculations. It is interesting that the vapor virtual mass velocities increase during passage through the tube in all three cases before decreasing to zero at the outlet.

The vapor phase virtual pressure gradient depends on the flow regime, i.e., viscous or turbulent, and the regime will change during passage through the tube. The pressure gradient is conventionally expressed in terms of the Fanning friction factor:

$$\left(\frac{\Delta P}{\Delta z}\right)_g = 2 \frac{f}{D_z\, g_c} \frac{G_g^{\,2}}{\rho_g} \tag{27}$$

The gradient is expressed here as a difference ratio rather than as a derivative because experimental data are actually obtained as differences.

For turbulent flow the friction factor may be expressed as:[2,5]

$$f = \frac{0.046}{N_{Rg}^{\;0.2}} \tag{28}$$

and for viscous flow:

$$f = \frac{16}{N_{Rg}} \tag{29}$$

Thus the turbulent vapor phase pressure gradient becomes:

$$\left(\frac{\Delta P}{\Delta z}\right)_{gt} = \frac{0.092}{D_z\, g_c} \frac{G_g^{\,2}}{\rho_g} \frac{1}{N_{Rg}^{\;0.2}} \tag{30}$$

and the viscous vapor phase pressure gradient is:

$$\left(\frac{\Delta P}{\Delta z}\right)_{gv} = \frac{32\, G_g^{\,2}}{D_z\, g_c\, \rho_g\, N_{Rg}} \tag{31}$$

The corresponding liquid virtual pressure gradient equations are identical to Eqs. 30 and 31 with substitution of the appropriate values for the liquid in place of the vapor values. Thus the flow moduli for the various combinations of flow regimes are obtained by substituting these equations in Eq. 2. The results are shown below, where the double subscripts refer to liquid and gas flow regimes in that order.

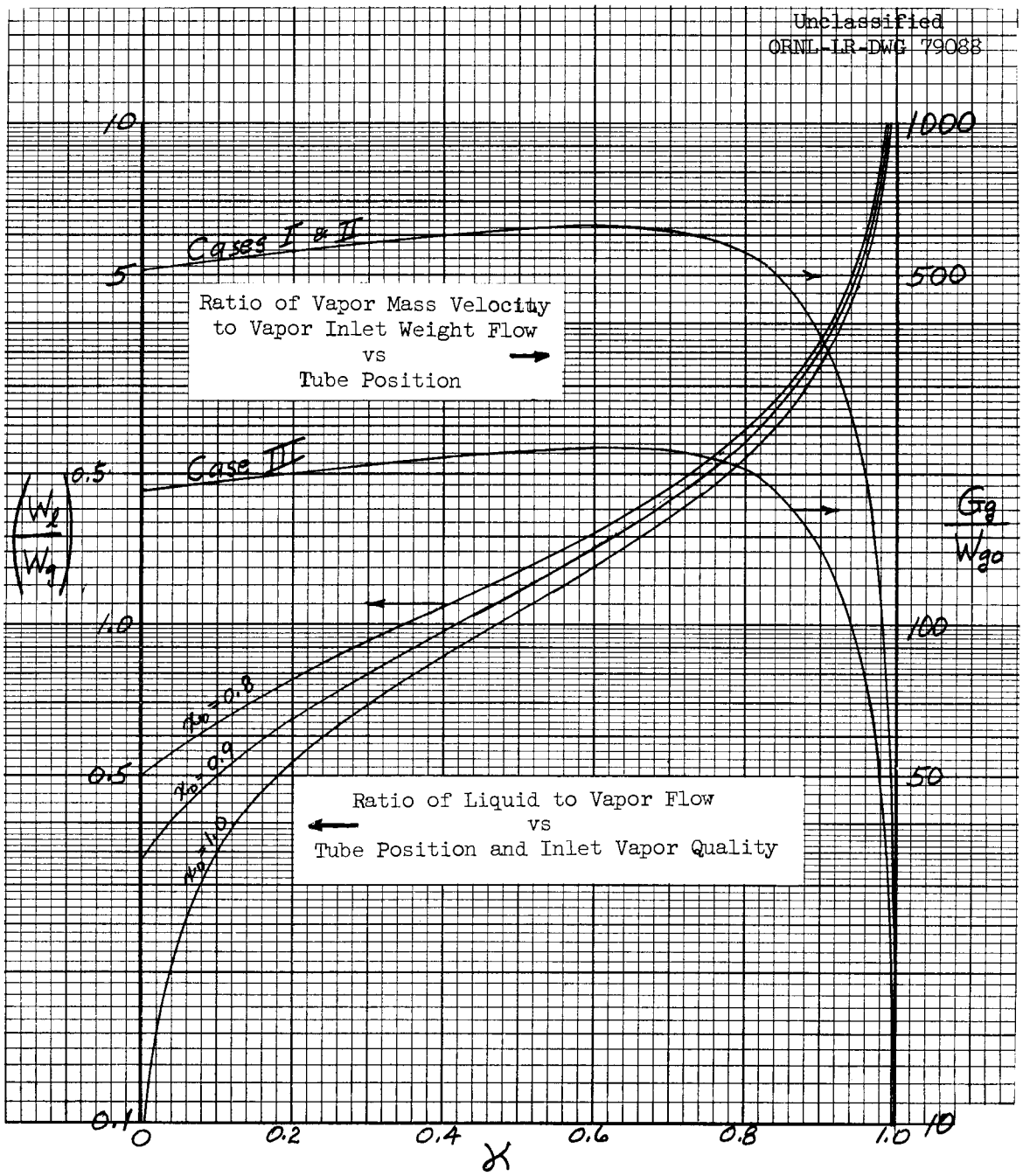

Fig. 3. Condensing Flow in Tapered Tubes at Constant Heat Flux.

$$X_{vv} = K \left[\frac{W_\ell}{W_g}\right]^{0.5} \tag{32}$$

where

$$K = \left[\frac{\rho_g \, \mu_\ell}{\rho_\ell \, \mu_g}\right]^{0.5} \tag{33}$$

$$X_{vt} = 18.7 \, K \left[\frac{W_\ell}{W_g}\right]^{0.5} \left[\frac{1}{N_{Rg}}\right]^{0.4} \tag{34}$$

$$X_{tv} = 0.0532 \, K \left[\frac{W_\ell}{W_g}\right]^{0.5} [N_{R_\ell}]^{0.4} \tag{35}$$

$$X_{tt} = K \left[\frac{W_\ell}{W_g}\right]^{0.5} \left[\frac{N_{R_\ell}}{N_{Rg}}\right]^{0.4} \tag{36}$$

The Reynolds numbers for the vapor and liquid virtual flows are shown in Fig. 4 vs tube position for the three cases. The transition from turbulent to viscous flow is, in fact, not clearly defined, and it extends approximately over the range of Reynolds numbers from 1000 to 2000.[1] Thus, clearly marked flow regimes exist only for vapor and liquid Reynolds numbers lying above and below the transition range. It therefore becomes necessary to assume that a given regime, initially well defined, continues to exist until the Reynolds numbers change sufficiently to define another regime clearly. On this basis Fig. 4 indicates that, for Cases I and II, the viscous liquid-turbulent vapor regime exists for about 90 to 95% of the tube length, whereupon the regime changes to turbulent liquid-viscous vapor. In Case III the viscous liquid-turbulent vapor regime changes to turbulent liquid-turbulent vapor at about 85 to 90% of the tube length, dropping to turbulent liquid-viscous vapor at some position beyond 95% of the tube length. These conclusions are illustrated in Fig. 5.

There is no way to determine theoretically how the actual, two-phase flow will match the model, but the model does provide a logical basis for analyzing experimental data in which the mismatch between model and reality is implicitly taken account of in a Lockhart-Martinelli type of correlation.

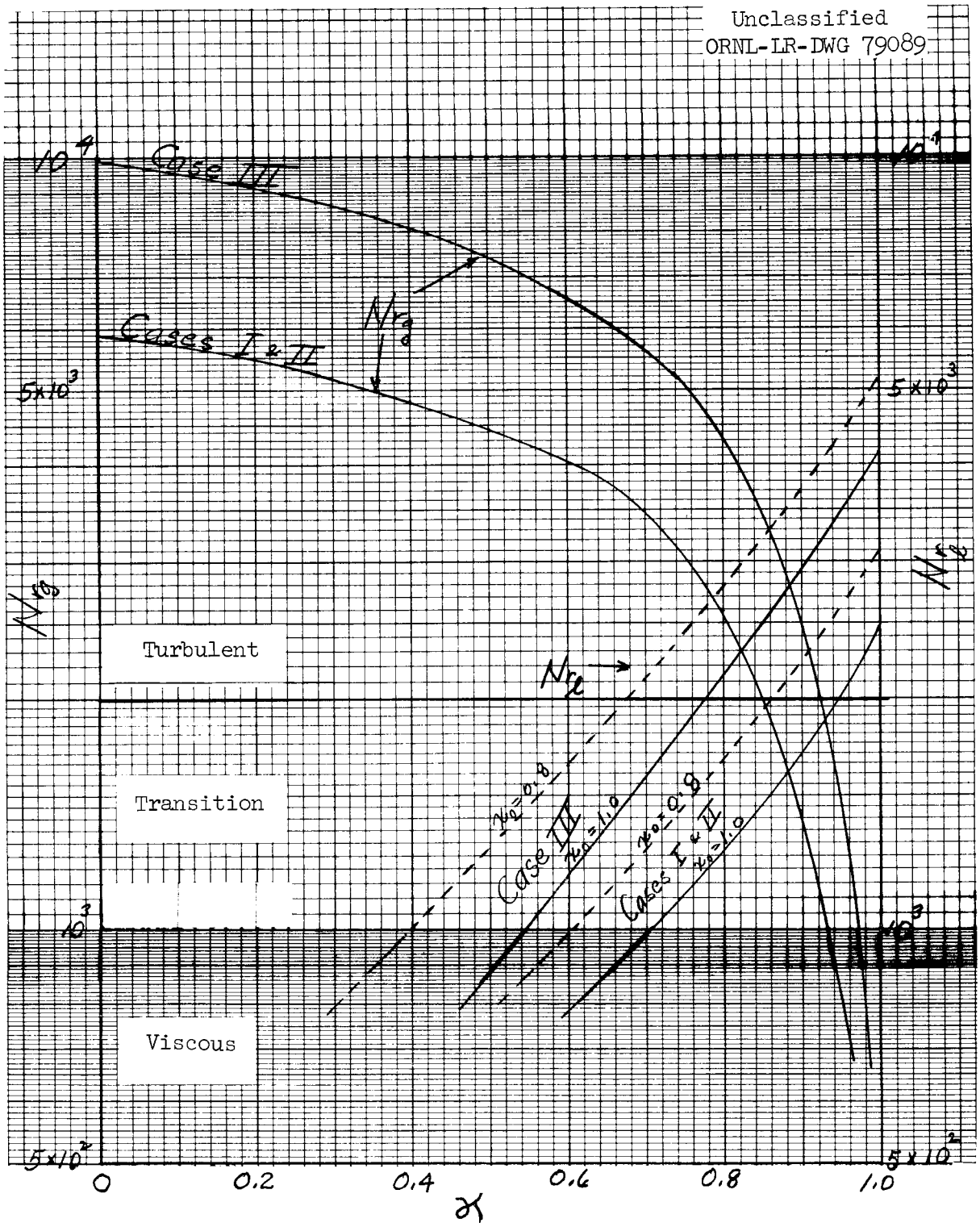

Fig. 4. Vapor and Liquid Reynolds Numbers vs Tube Position for Condensing Potassium in Finned, Tapered Tubes at 1500°R (1040°F).

Unclassified
ORNL-LR-DWG 79090

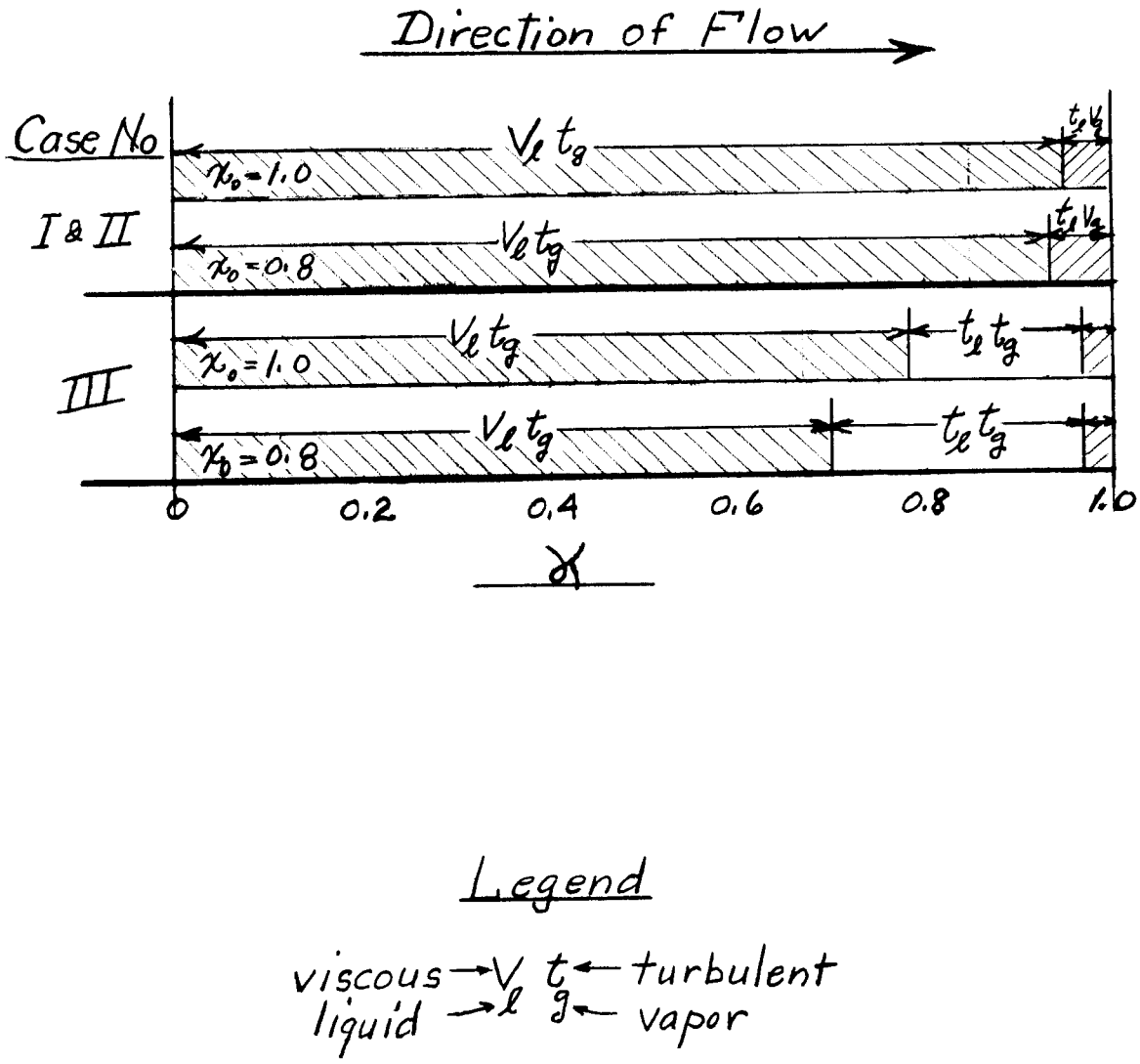

Fig. 5. Distribution of Flow Regimes in the Condensing Tube Based on Single Component Flow.

The single-phase flow moduli corresponding to the regimes illustrated in Fig. 5 are plotted in Figs. 6 and 7 for inlet vapor qualities of 1.0 and 0.8 respectively. The X_{tv} regime is omitted because the pressure drop in the last few per cent of the tube is negligible.

The vapor phase virtual pressure gradients for the three cases are plotted against tube position in Figs. 8 and 9 (lower curves). In all cases the gradient rises rather steeply to a peak occurring about 80% down the tube. This peak appears to be characteristic of condensing flow in tapered tubes with high inlet vapor velocity. On passing the peak the gradient falls rapidly and eventually passes into the viscous vapor flow regime.

In order to calculate the actual, two-phase friction pressure drop, an empirical correlation of ϕ^2 vs X is required. Such data for potassium are not currently available, but the fair success of Baroczy and Sanders[2] in applying their nitrogen-mercury flow correlation to condensing steam flow suggests that a similar application to condensing potassium might not be too greatly in error, at least for preliminary design considerations. The correlation is shown in Fig. 10. Using this correlation, the calculated two-phase friction pressure drops for the three cases are shown in Figs. 8 and 9 (upper curves). In Fig. 9 the transition from viscous liquid-turbulent vapor to both phases turbulent is indicated by the cross-hatched areas. The corresponding transition for Fig. 8 occurs about 95% down the tube where the gradient drops too rapidly for the change in slope to be apparent.

Momentum Pressure Recovery

Accompanying the condensing process is a change in momentum which results in a pressure recovery, thus offsetting the friction drop to some extent.[2]

The momentum equation for an open system is as follows:[6]

$$F = \frac{\dot{m}}{g_c} (\overline{V}_e - \overline{V}_i) \tag{37}$$

where $\dot{m}$ is the mass flow through the system and the $\overline{V}$'s are the exit and entering velocities. In present nomenclature the equation becomes:

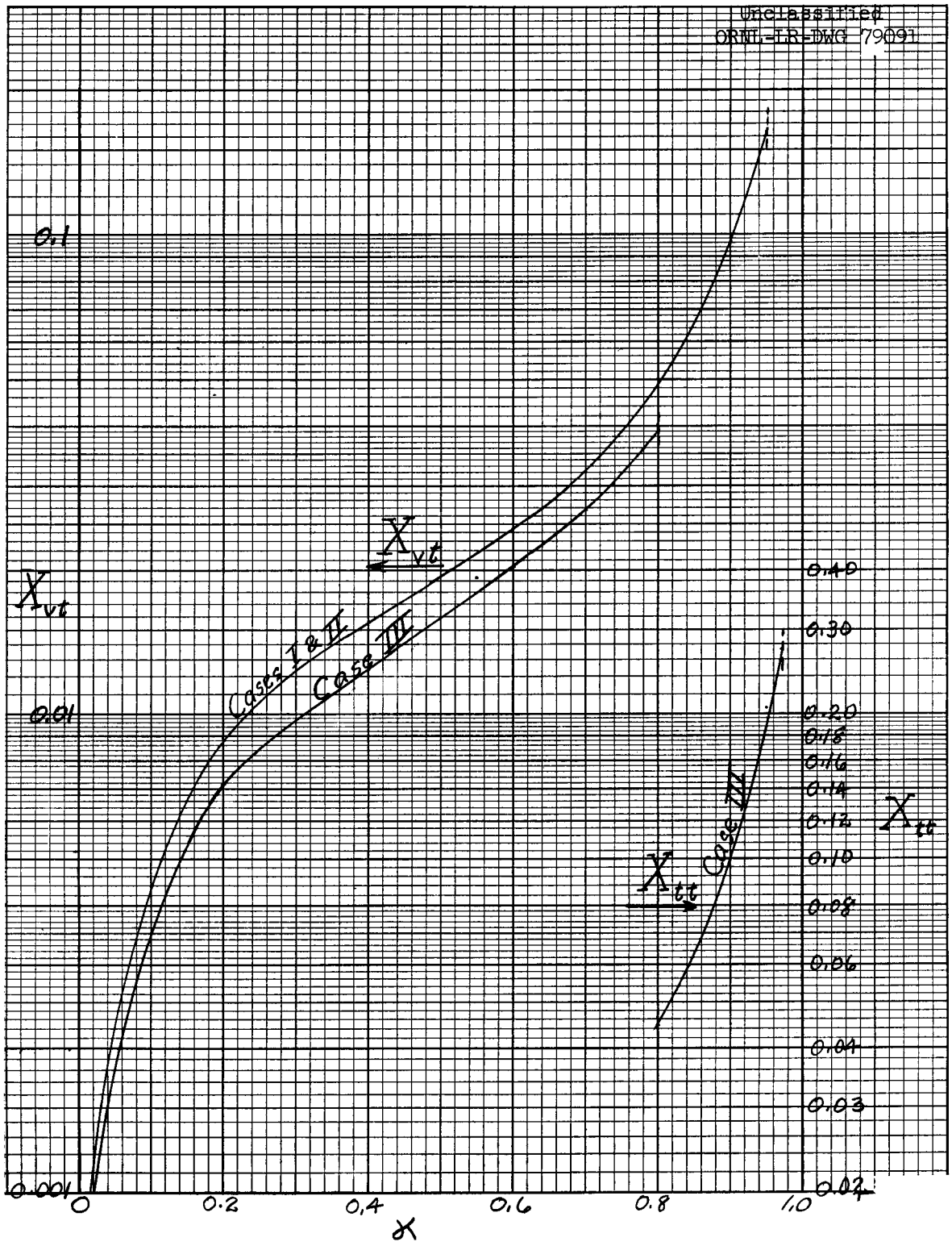

Fig. 6. Single Phase Flow Moduli, x_o = 1.0, for Condensing Potassium in Finned, Tapered Tubes at 1500°R (1040°F).

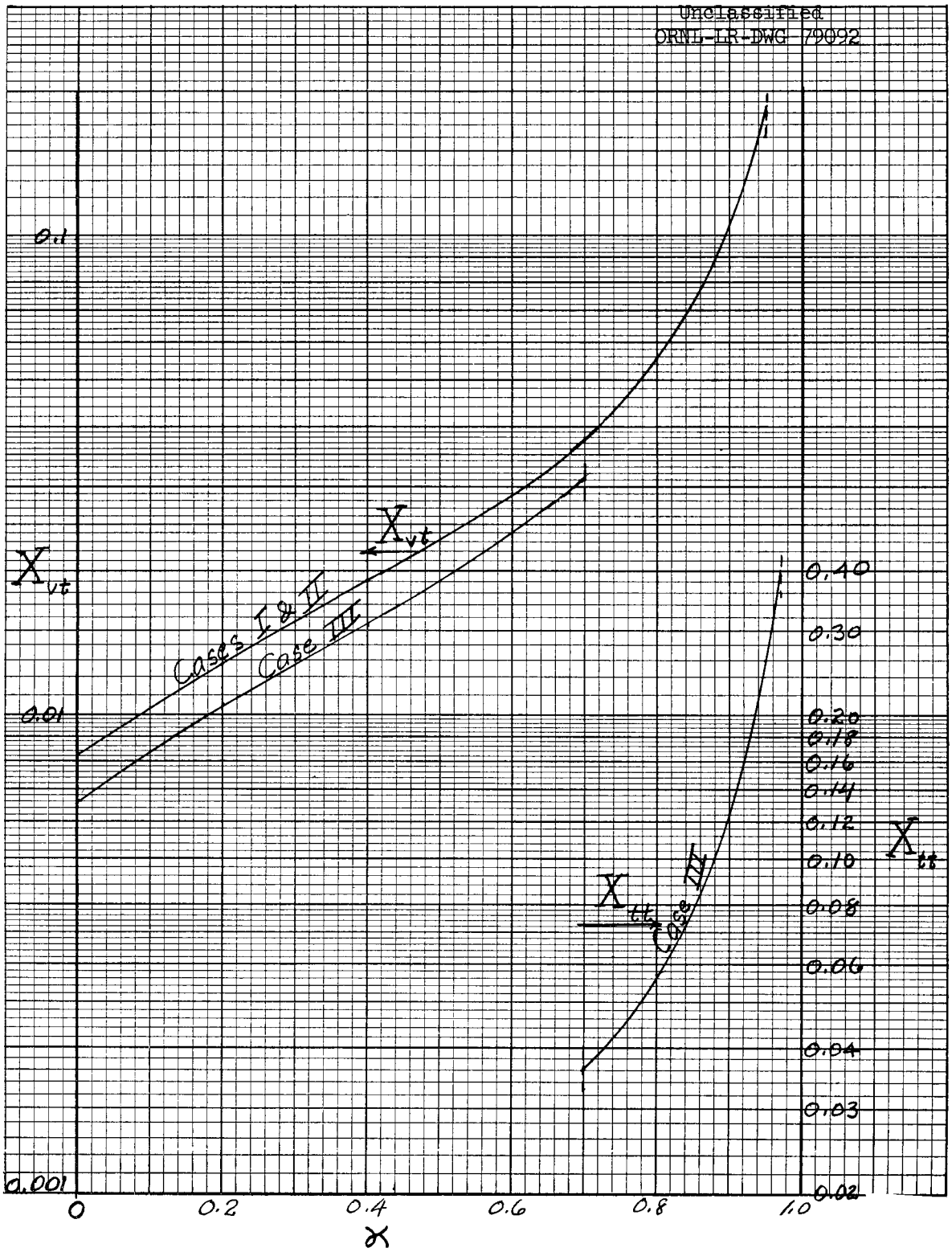

Fig. 7. Single Phase Flow Moduli, x_o = 0.8, for Condensing Potassium in Finned, Tapered Tubes at 1500°R (1040°F).

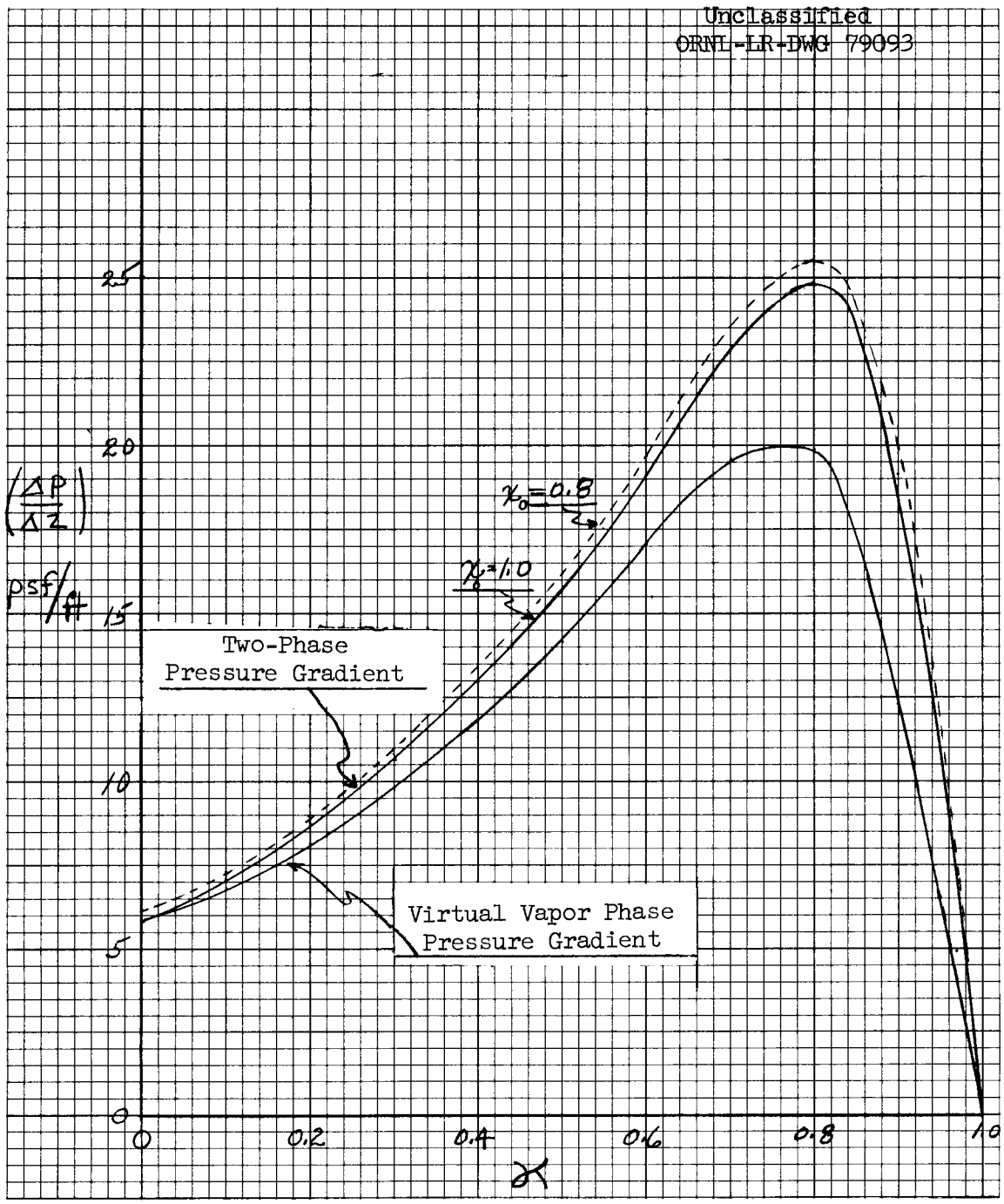

Fig. 8. Two-Phase Friction Pressure Gradient vs Normalized Tube Length for Condensing Potassium in Finned, Tapered Tubes at 1500°R (1040°F), Cases I and II.

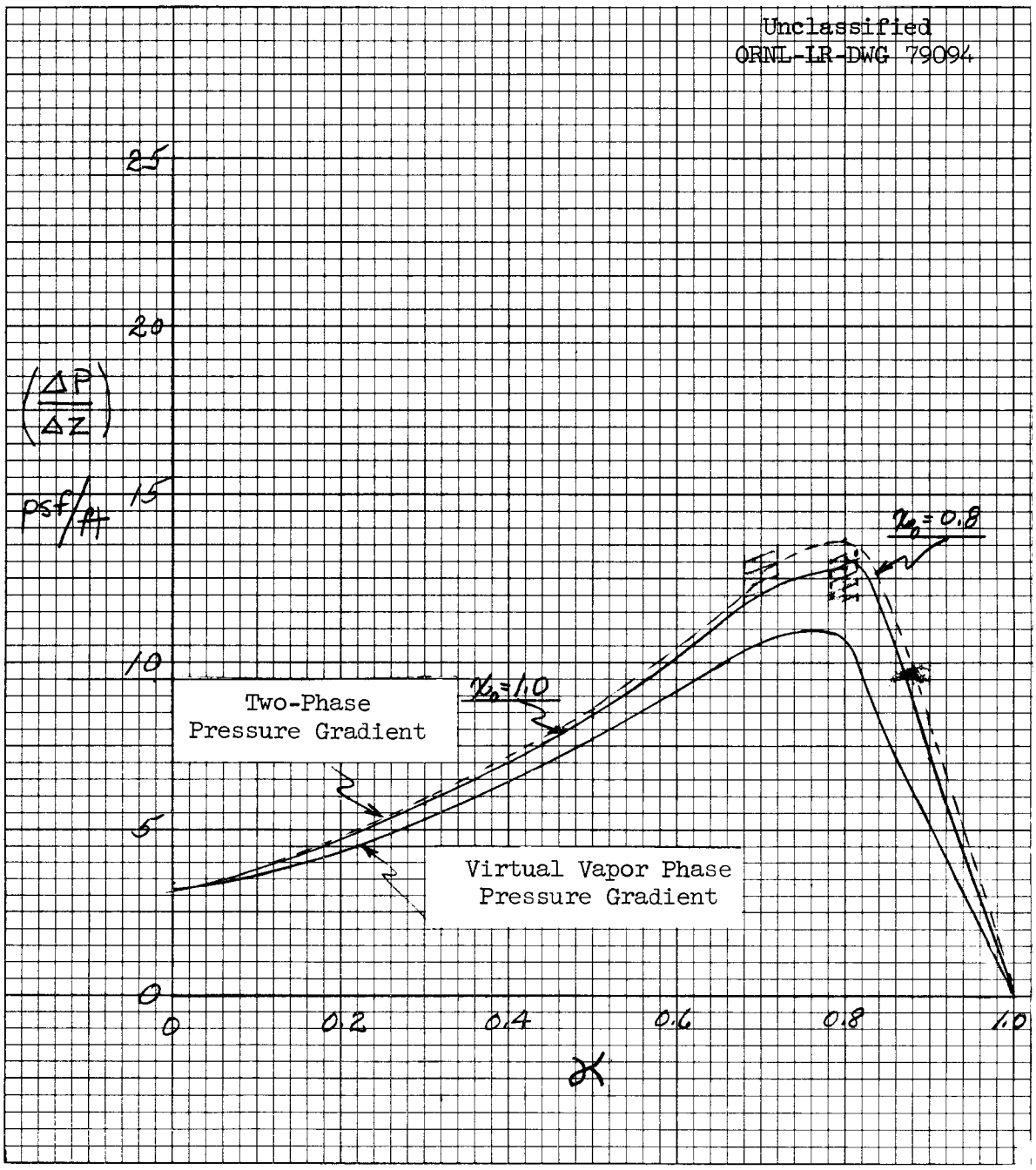

Fig. 9. Two-Phase Friction Pressure Gradient vs Normalized Tube Length for Condensing Potassium in Finned, Tapered Tubes at 1500°R (1040°F), Case III.

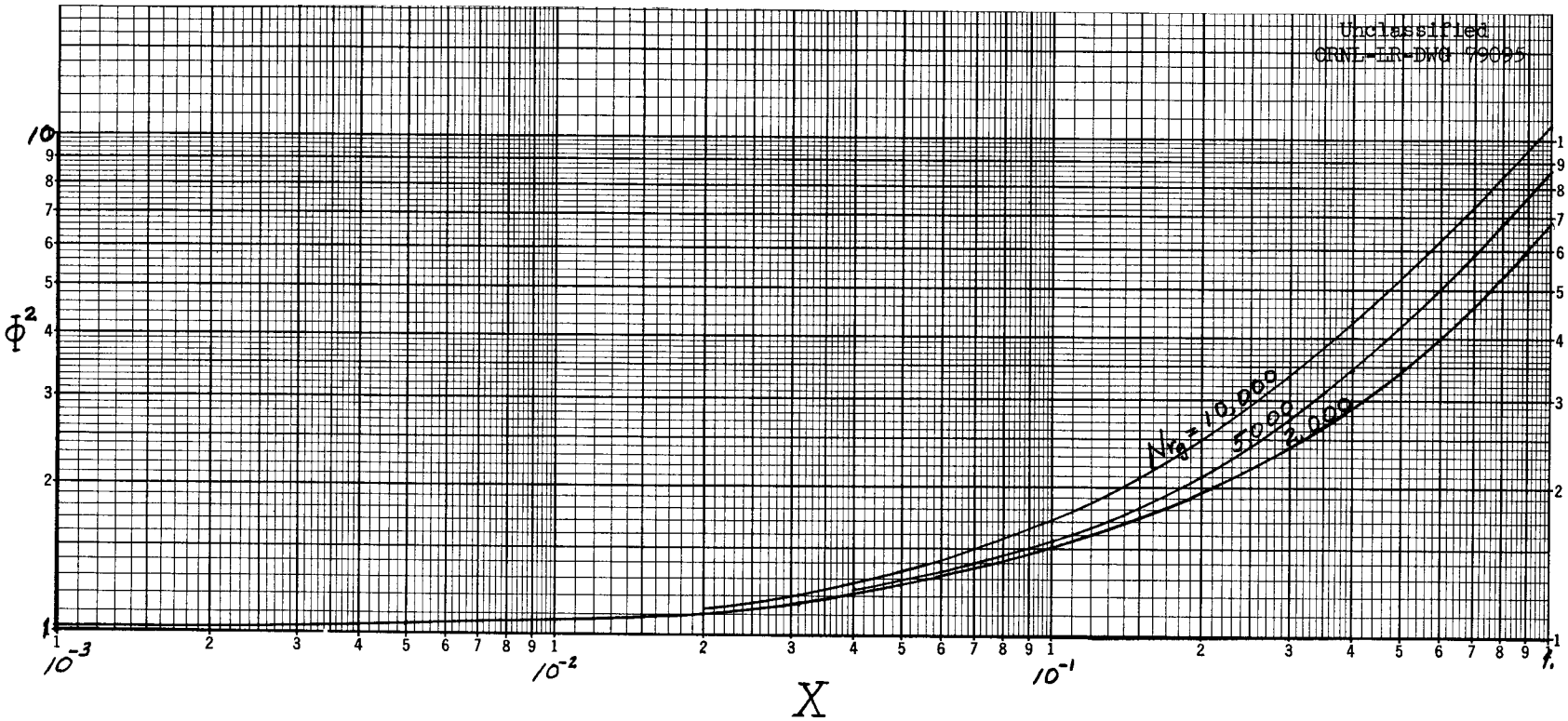

Fig. 10. General Correlation for Two-Phase, Two-Component Pressure Drop. See Baroczy and Sanders.[2]

$$F = \frac{W_{g_o}}{x_o \; g_c} (- V_{g_o}) \tag{38}$$

since the liquid velocity is negligible compared to the vapor. To obtain the pressure recovery, divide both sides by the cross-sectional area:

$$\Delta P_{mL} = \frac{- W_{g_o}}{A_o \; x_o \; g_c} V_{g_o} = \frac{- W_{g_o}^{\;2}}{A_o^{\;2} \; x_o \; g_c \; \rho_{g_o}} \tag{39}$$

Since one cannot assume that the liquid entrainment in entering vapors of low quality will necessarily flow at the same high velocity as the vapor, a more conservative approach is to neglect the entrainment momentum entirely by letting $x_o = 1$. The calculated pressure recovery will then be low.[2]

The momentum pressure gradient is obtained by differentiating Eq. 39 expressed in general terms:

$$\frac{d}{dz} (\Delta P_{mz}) = \frac{1}{g_c} \frac{d}{dz} \left[\left(\frac{W_g}{\rho_g} \right)^2 \left(\frac{1}{A_z} \right)^2 \right] = \frac{1}{g_c} \frac{d}{dz} \left[\frac{G_g^{\;2}}{\rho_g} \right] \tag{40}$$

$$\frac{d}{dz} (\Delta P_{mz}) = \left[\frac{2G_g}{\rho_g} \left(\frac{d \; G_g}{dz} \right) - \frac{G_g^{\;2}}{\rho_g^{\;2}} \left(\frac{d \; \rho_g}{dz} \right) \right] \tag{41}$$

In cylindrical tubes with uniform condensation rate,

$$A_z = A_o$$

$$W = W_{g_o} (1 - \kappa)$$

and

$$\frac{dW}{dz} = - \frac{W_{g_o}}{L}$$

$$\frac{d}{dz} (\Delta P_{mz}) = \frac{- W_{g_o}^{\;2}}{A_o^{\;2} \; g_c \; \rho_g} (1 - \kappa) \left[\frac{2}{L} + \frac{1}{\rho_g} (1 - \kappa) \left(\frac{d \; \rho_g}{dz} \right) \right] \tag{42}$$

It is not apparent that the variation in ρ_g with z can be neglected

since the condensing pressure drop is a significant fraction of the inlet pressure. If it is neglected, however,

$$\frac{d}{dz}(\Delta P_{mz}) = \frac{-2\,W_{g_o}^{\;2}}{A_o^{\;2}\,g_c\,\rho_g\,L}(1-\kappa) = \frac{-2\,\Delta P_{mL}}{L}(1-\kappa) \tag{43}$$

which is the Baroczy and Sanders equation.[2] On integration from 0 to κ, this equation yields:

$$\frac{\Delta P_{mz}}{\Delta P_{mL}} = \kappa\,(2-\kappa) \tag{44}$$

If one supposes that ρ_g varies linearly with z, Eq. 42 can be integrated by parts. Let

$$\rho_g = \rho_{go}\,(1-\omega\,\kappa)$$

$$\frac{d}{d\kappa}(\Delta P_{mz}) = \Delta P_{mL}\left(\frac{1-\kappa}{1-\omega\kappa}\right)\left[2-\frac{\omega\kappa\,(1-\kappa)}{1-\omega\,\kappa}\right] \tag{45}$$

and

$$\begin{aligned}\frac{\Delta P_{mz}}{\Delta P_{mL}} = &-\frac{2}{\omega}\,\ell n\,(1-\omega\kappa) + \frac{2}{\omega}\left[\kappa + \frac{1}{\omega}\,\ell n\,(1-\omega\kappa)\right] \\ &-\frac{1}{\omega}\left[\frac{1}{1-\omega\kappa} + \ell n\,(1-\omega\kappa) - 1\right] \\ &-\frac{2}{\omega^2}\left[(1-\omega\kappa) - \frac{1}{1-\omega\kappa} - 2\,\ell n\,(1-\omega\kappa)\right] \\ &-\frac{\kappa}{\omega^2}\left[\frac{\omega\kappa}{2} + \frac{1}{1-\omega\kappa} + 2\,\ell n\,(1-\omega\kappa)\right] \\ &-\frac{1}{\omega^3}\left[(3-2\omega\kappa)\,\ell n\,(1-\omega\kappa) - 2\,(1-\omega\kappa) + 2\right]\end{aligned} \tag{46}$$

If the pressure drop across the tube (and hence the change in vapor density) does not exceed about 30% of the inlet pressure, the difference in the normalized pressure recovery from that calculated with constant density at inlet conditions is almost negligible. The two values are plotted against κ in Fig. 11. Consequently, the density derivative term in Eq.

Unclassified
ORNL-LR-DWG 79096

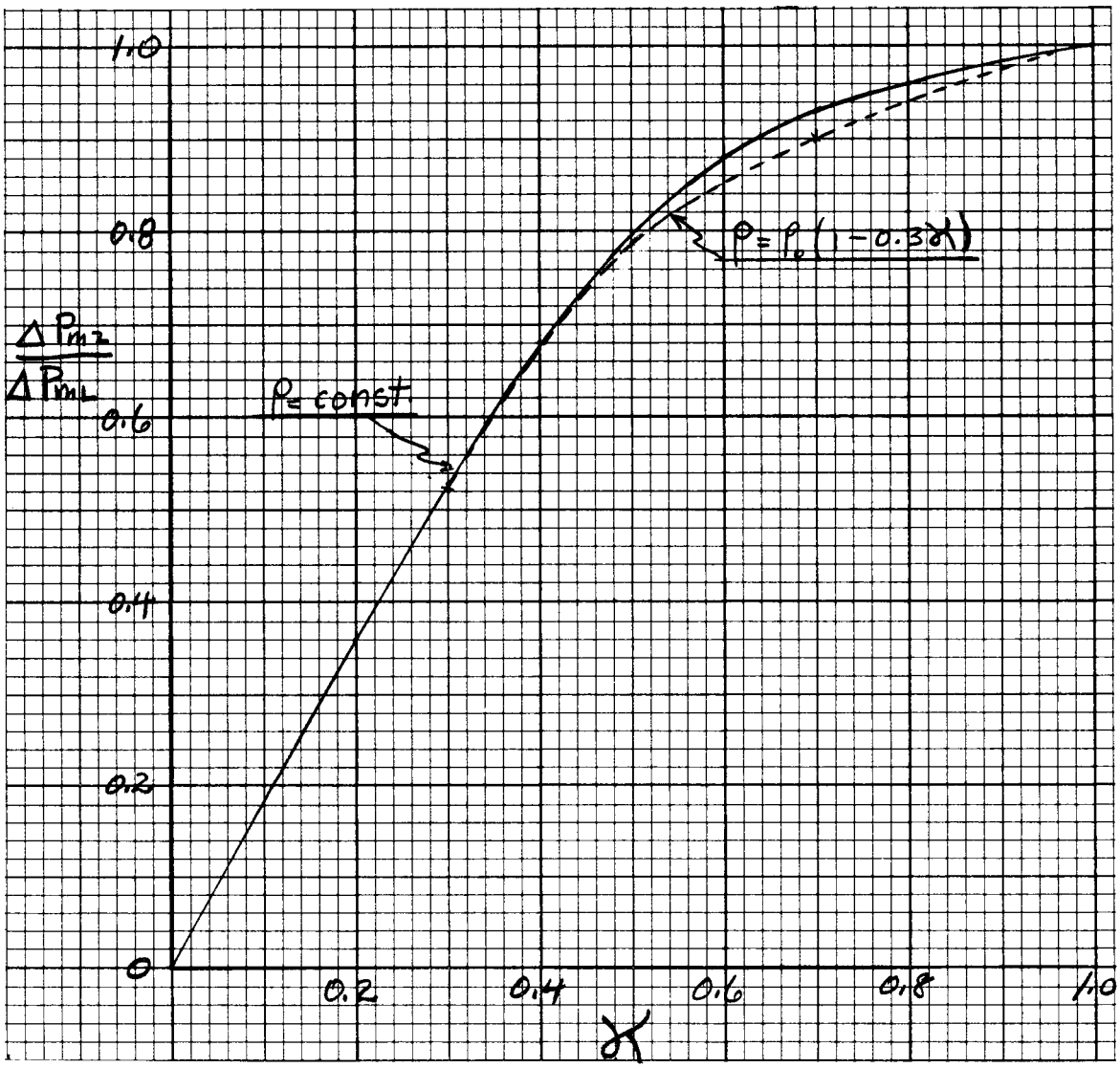

Fig. 11. Effect of Local Density on Momentum Pressure Recovery in Cylindrical Tubes.

42 is dropped for the calculations of Cases I and III. Although the density derivative is not negligible for Case II, the total pressure drop is well over half of the inlet pressure, and the entire two-phase correlation is of questionable application. For this reason, the condensing pressure drops are calculated for only Cases I and III.

The pressure recovery at z is, of course, the difference between that on total condensation and that remaining as the vapor stream momentum:

$$\Delta P_{mz} = \Delta P_{mL} - \left(\frac{- W_{g_z}^{2}}{A_z^{2} \; g_c \; \rho_{gz}} \right) \tag{47}$$

From Eqs. 22, 23, and 25 the normalized pressure recovery becomes:

$$\frac{\Delta P_{mz}}{\Delta P_{mL}} = 1 - \left[\frac{1 - 1.11 \, \kappa + 0.10 \, \kappa^2}{1 - 0.75 \, \kappa} \right]^2 \tag{48}$$

for the cases considered.

Equations 44 and 48 are plotted vs κ in Fig. 12. In the tapered tubes considered, it is apparent that the rate of momentum recovery is considerably distorted from that of a cylindrical tube.

Over-All Condensing Pressure Drop

The over-all, or net, pressure drop during condensing flow (ΔP_c) is the difference between the two-phase friction drop (ΔP_{TP}) and the momentum recovery (ΔP_m). All three of these quantities are plotted vs κ in Fig. 13 for Cases I and III. The two cases are nearly indistinguishable, so that one set of curves suffices for both.

Parallel Flow Stability

Since a space radiator of any practical size must contain many tapered tubes in parallel, it is conceivable that unstable conditions might exist whereby the flow through one tube (or group of tubes) could be blocked by the higher flow in others brought about by random flow perturbations.

Since the condensing pressure drop, ΔP_c, is a difference between the friction drop, ΔP_{TP} (plus entrance and exit losses), and the momentum pressure recovery, ΔP_m, instability will arise whenever the rate of

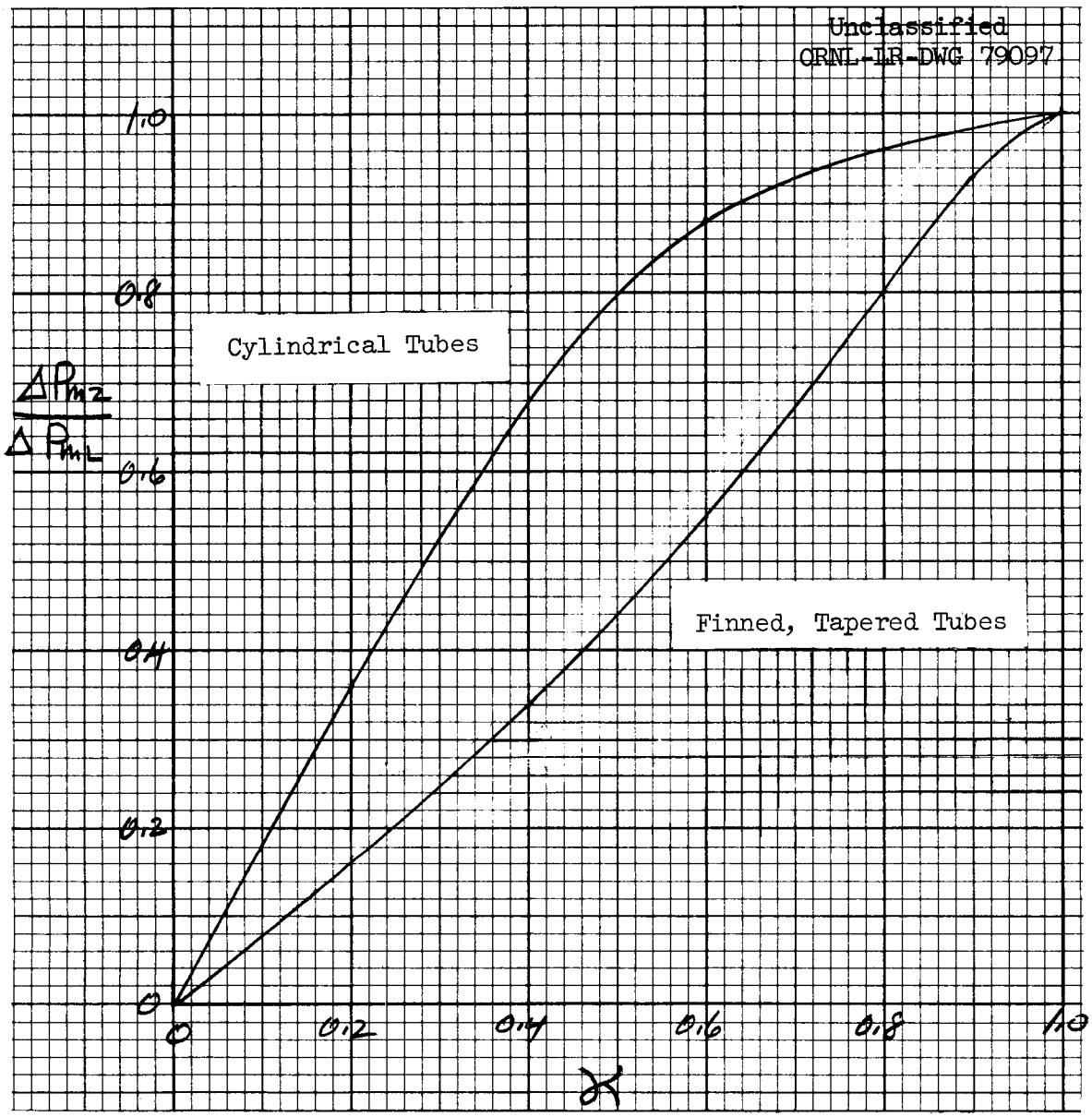

Fig. 12. Normalized Momentum Recovery vs Normalized Tube Length.

Unclassified
ORNL-LR-DWG 79098

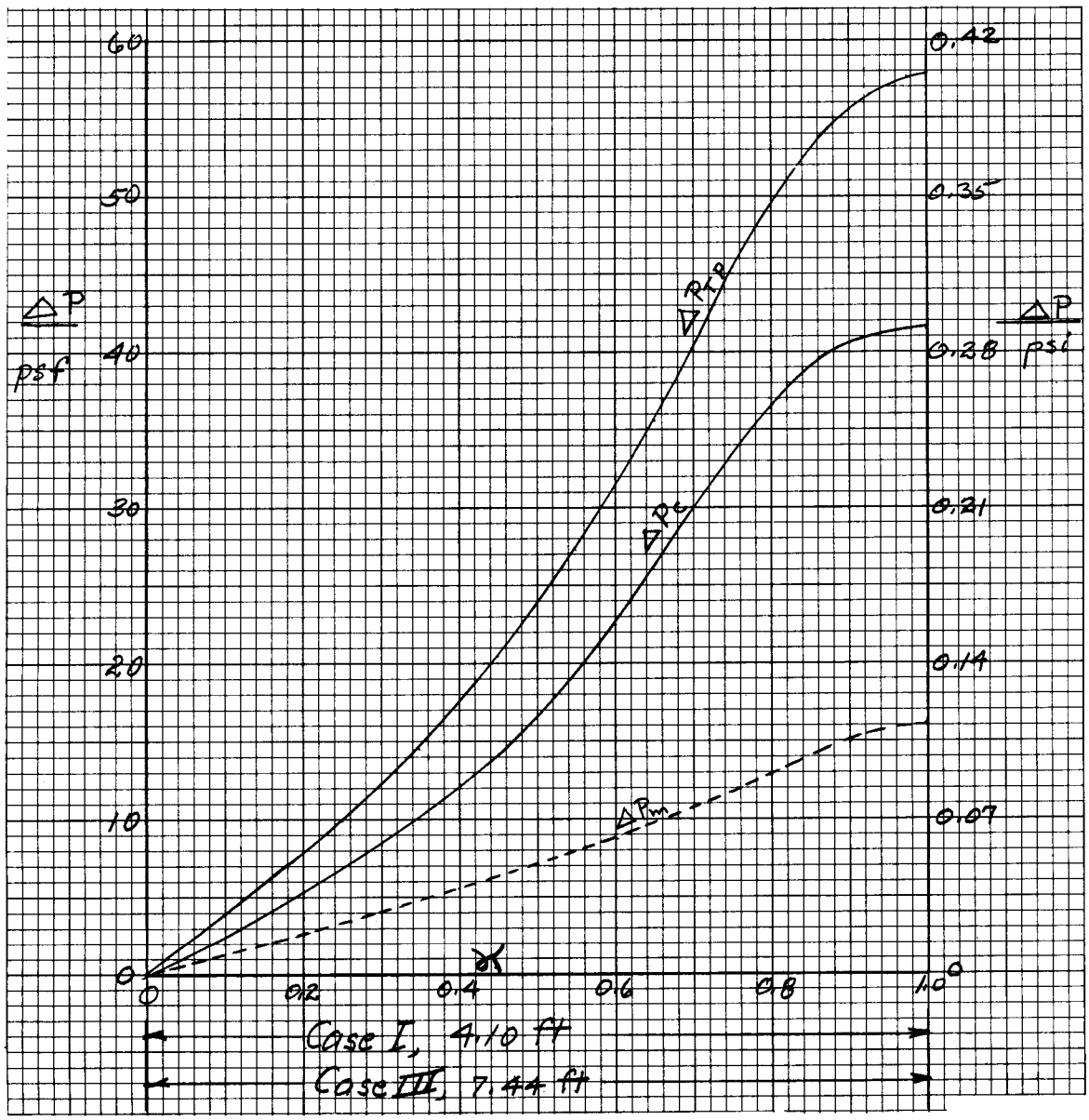

Fig. 13. Condensing Potassium in Finned, Tapered Tubes at 1500°R (1040°F). Cases I and III, x_o = 1.0.

change of ΔP_c with respect to inlet mass flow, $d\Delta P_c/dw_{go}$, is negative. A "metastable" condition could arise even when the rate of change is positive if ΔP_m exceeds ΔP_{TP}, resulting in a higher condensate manifold pressure than inlet manifold pressure. However, large flow perturbations would be required to bring about instability in this case.

An analysis of this instability problem has been undertaken by Kunz, Ornstein, Wyde, and Hooper[7] for condensing flow in cylindrical tubes at constant heat flux. In order to render the mathematics more tractable they assumed that the friction pressure drop was always equal to the product of the vapor pressure gradient at the inlet, $(\Delta P/\Delta z)_g$, and the condensation length, λ. This assumption could produce significant error, as they have pointed out. However, their further analysis indicates that the assumption probably does not introduce serious error, insofar as cylindrical tubes are concerned. The final proof, of course, will be that obtained experimentally.

In the case of condensing flow in tapered tubes one would not expect the friction pressure drop necessarily to be equal to $(\Delta P/\Delta z)_g \lambda$ in view of the wide range of the friction pressure gradient along the tube (see Figs. 8 and 9). Without this assumption, however, there is no simple way to extend the analysis in general terms, and comparison is made only by examination of specific examples. To do this the general equations for heat transfer surface, ratio of liquid-to-vapor flow, Reynolds numbers, single-phase flow moduli, pressure gradient, etc., previously expressed in terms of the normalized tube length, κ, must be restated in terms of a new parameter, ψ, which is the inlet vapor flow normalized with respect to design inlet vapor flow, (w_{go}/W_{go}), since the tube dimensions are now fixed.

Choosing initial, or design, conditions (P, T_c, W_{go}, Q/A) for condensation over the entire tube length, L, the reduced inlet flow at the same Q/A and P establishes the following conditions:

$$\frac{w_{go}}{W_{go}} = \psi = \frac{A_{h\lambda}}{A_{hL}} \qquad \text{(A)}$$

From Eq. 21:

$$\frac{w_\ell}{w_g} = \frac{1}{x_o\left(1 - \frac{A_{hz}}{A_{h\lambda}}\right)} - 1 \tag{21-A}$$

From Eq. 23:

$$\frac{A_{hz}}{A_{h\lambda}} = \frac{1}{\psi}\left(1.11\,\kappa - 0.10\,\kappa^2\right) \tag{23-A}$$

$$\frac{w_\ell}{w_g} = \left[\frac{1}{x_o\left[1 - \frac{1}{\psi}\left(1.11\,\kappa - 0.10\,\kappa^2\right)\right]} - 1\right] \tag{24-A}$$

From Eq. 22:

$$\frac{G_g}{w_{g_o}} = \frac{1}{A_z}\left(1 - \frac{A_{hz}}{A_{h\lambda}}\right) \tag{22-A}$$

$$\frac{G_g}{w_{g_o}} = \frac{4}{\pi D_o^2\,(1 - \alpha\kappa)^2}\left[1 - \frac{1}{\psi}\left(1.11\,\kappa - 0.10\,\kappa^2\right)\right] \tag{26-A}$$

For specific comparison, the tube design and initial conditions of Case I were chosen, and a plot of G_g/w_{go} vs κ for different ratios of reduced flow (with design value of Q/A_{hx} = 5960 Btu/hr·ft^2 <u>external</u> surface) is shown in Fig. 14. Along with the plot is a curve showing the normalized condensing length (the value of κ) corresponding to the reduced flow ratio, ψ. For cylindrical tubes, where Q/L is constant, the reduced flow ratio equals the normalized condensing length, as shown by the dotted line. The deviation of the solid curve from the dotted line shows the effect of the tube taper.

Similarly, the liquid-to-vapor weight flow ratios for inlet vapor qualities of 1.0 and 0.8 at different reduced flows are shown in Fig. 15 vs κ. Figures 14 and 15 are analogous to Fig. 3.

The single-phase vapor and liquid Reynolds numbers are shown in Fig. 16 as functions of κ and ψ. The vapor Reynolds numbers are continuous functions of κ for each value of ψ, dropping to zero when κ equals the normalized condensation length, λ/L. The liquid Reynolds

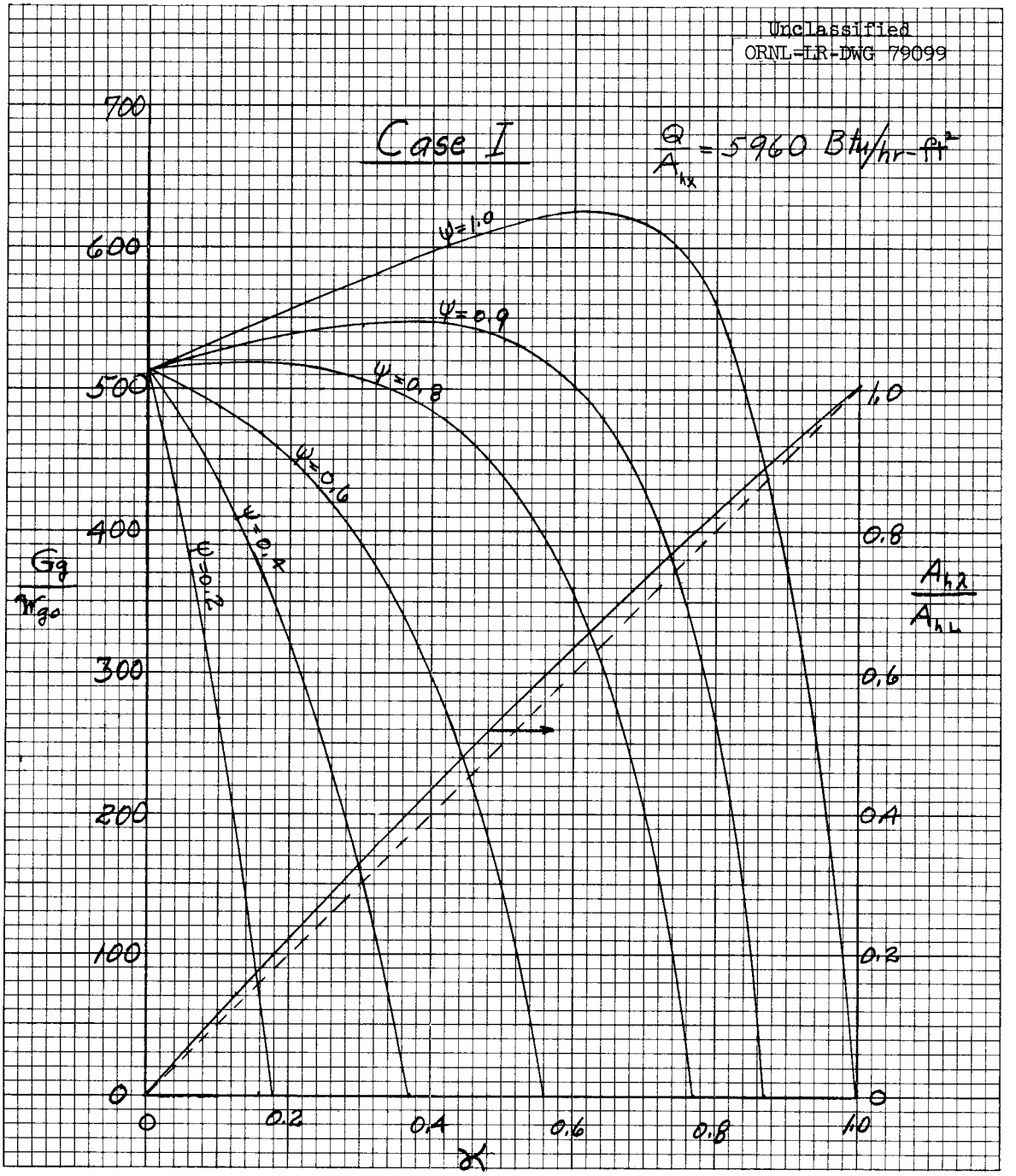

Fig. 14. Ratio of Vapor Mass Velocity to Vapor Inlet Weight Flow vs Tube Position for Condensing Flow in Tapered Tubes at Constant Heat Flux.

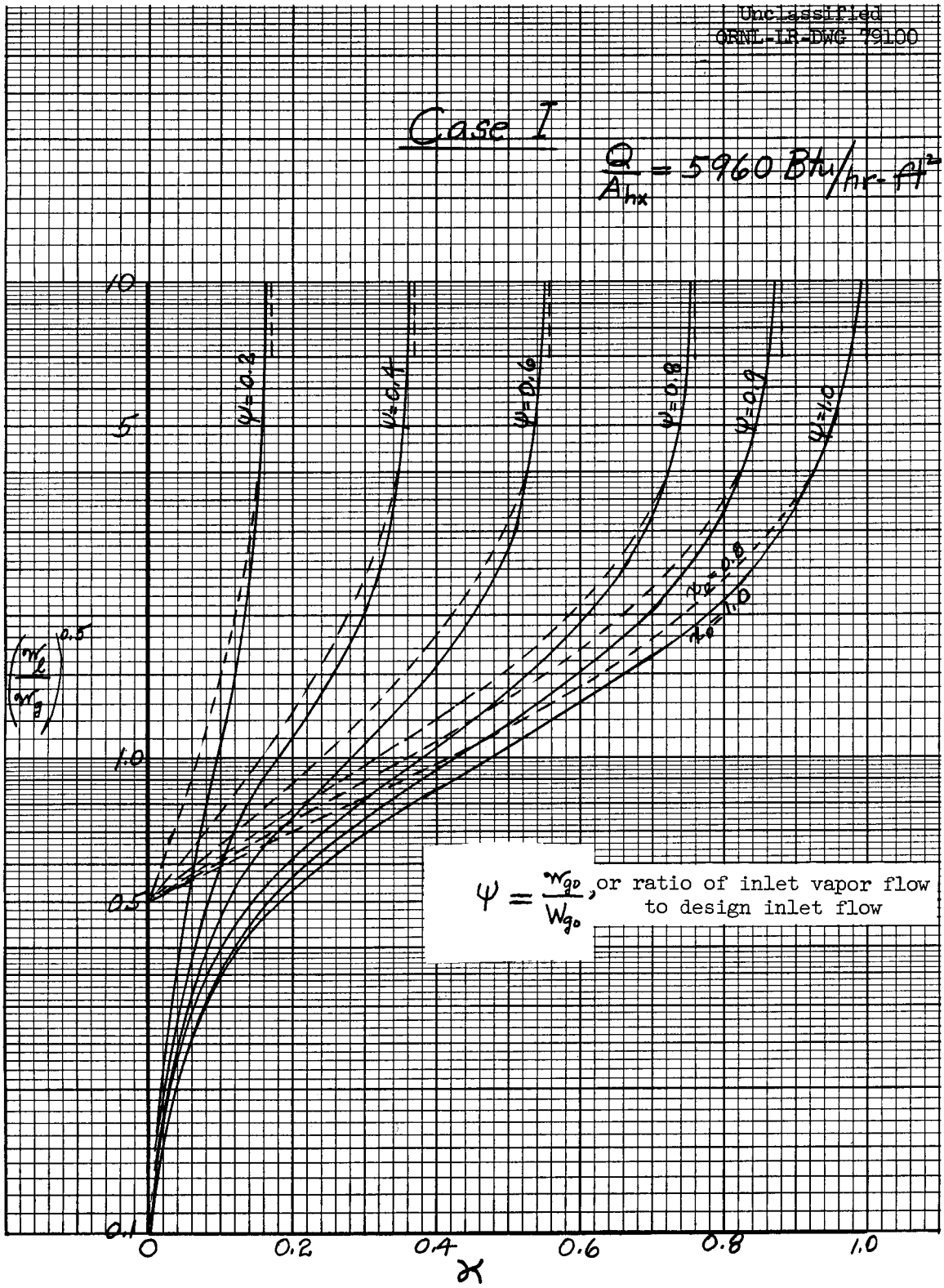

Fig. 15. Ratio of Liquid to Vapor Flow vs Tube Position for Condensing Flow in Tapered Tubes at Constant Heat Flux.

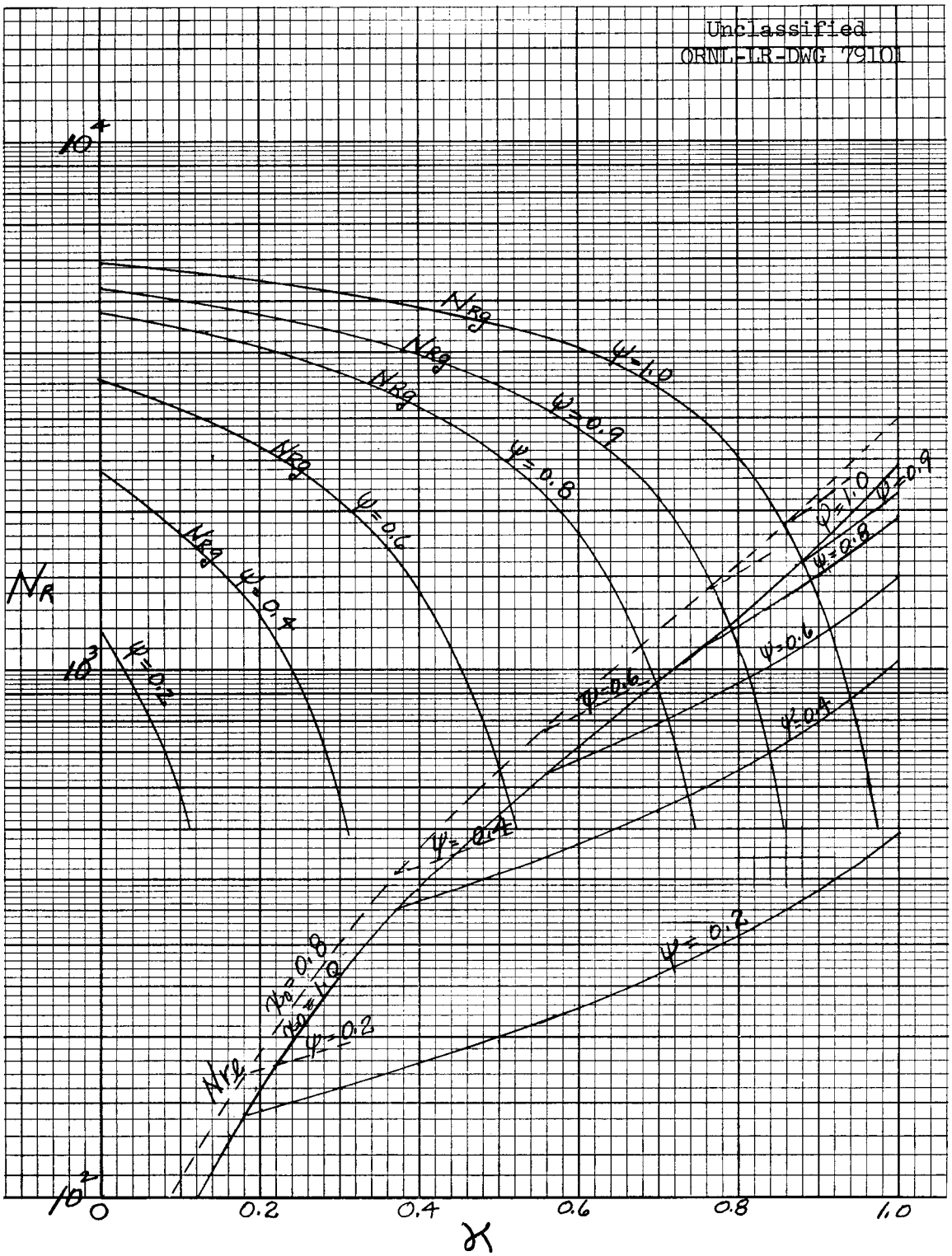

Fig. 16. Reynolds Number vs Tube Position for Reduced Flows at Constant Heat Flux in Condensing Potassium at 1500°R, Case I.

numbers, however, lie in a continuous, single curve over the condensation length (for any given vapor inlet quality, x_o), breaking away from that curve for values of κ greater than λ/L, for in this region the tube is flowing full of liquid. Figure 16 is analogous to Fig. 4.

The only flow modulus that need be considered for reduced inlet flow is the viscous-liquid, turbulent-vapor flow, X_{vt}. It is shown in Fig. 17 as a function of κ, ψ, and x_o, corresponding to the X_{vt} regime of Figs. 6 and 7.

From Eq. 30 the values of $(\Delta P/\Delta z)_g$ were calculated vs κ for selected values of ψ, over the range of κ up to the point where N_{Rg} dropped down to 1000, or slightly short of where $\kappa = \lambda/L$. Using the Lockhart-Martinelli correlation shown in Fig. 10, the two-phase pressure gradient was estimated over the same range of κ and the two-phase pressure drop, ΔP_{TP}, obtained by summation. The all-liquid pressure drop in that part of the tube beyond condensation is negligible.

The momentum pressure recovery was calculated directly from Eq. 39, recognizing that the inlet vapor weight flow depends on ψ:

$$\Delta P_m = \frac{- w_{go}^2}{A_o^2 \; x_o \; g_c \; \rho_{go}} \qquad (39\text{-A})$$

The difference between ΔP_{TP} and ΔP_m is shown as ΔP_c in Fig. 18 as a function of ψ for inlet vapor qualities of $x_o = 1.0$ and $x_o = 0.8$. The curve for $x_o = 0.8$ is rather extreme in that the velocity of the entering entrainment was assumed to be equal to the vapor velocity. The true curve lies much closer to that shown for $x_o = 1.0$. It is immediately apparent that there are two values of inlet vapor flow (less than the chosen design flow) at which the condensing pressure drop is zero. The first value is obviously zero flow, and the second value occurs at about 75 and 90% of the design inlet vapor flow for inlet vapor qualities of 1.0 and 0.8 respectively. In their stability analysis, Kunz, et al., used this flow (where $\Delta P_{TP} = \Delta P_m$) as the datum for determining the relative flow at which the condensing pressure drop is minimum, and at this latter flow there is a net pressure increase from inlet to outlet of the tube. For cylindrical tubes this minimum occurs at a flow

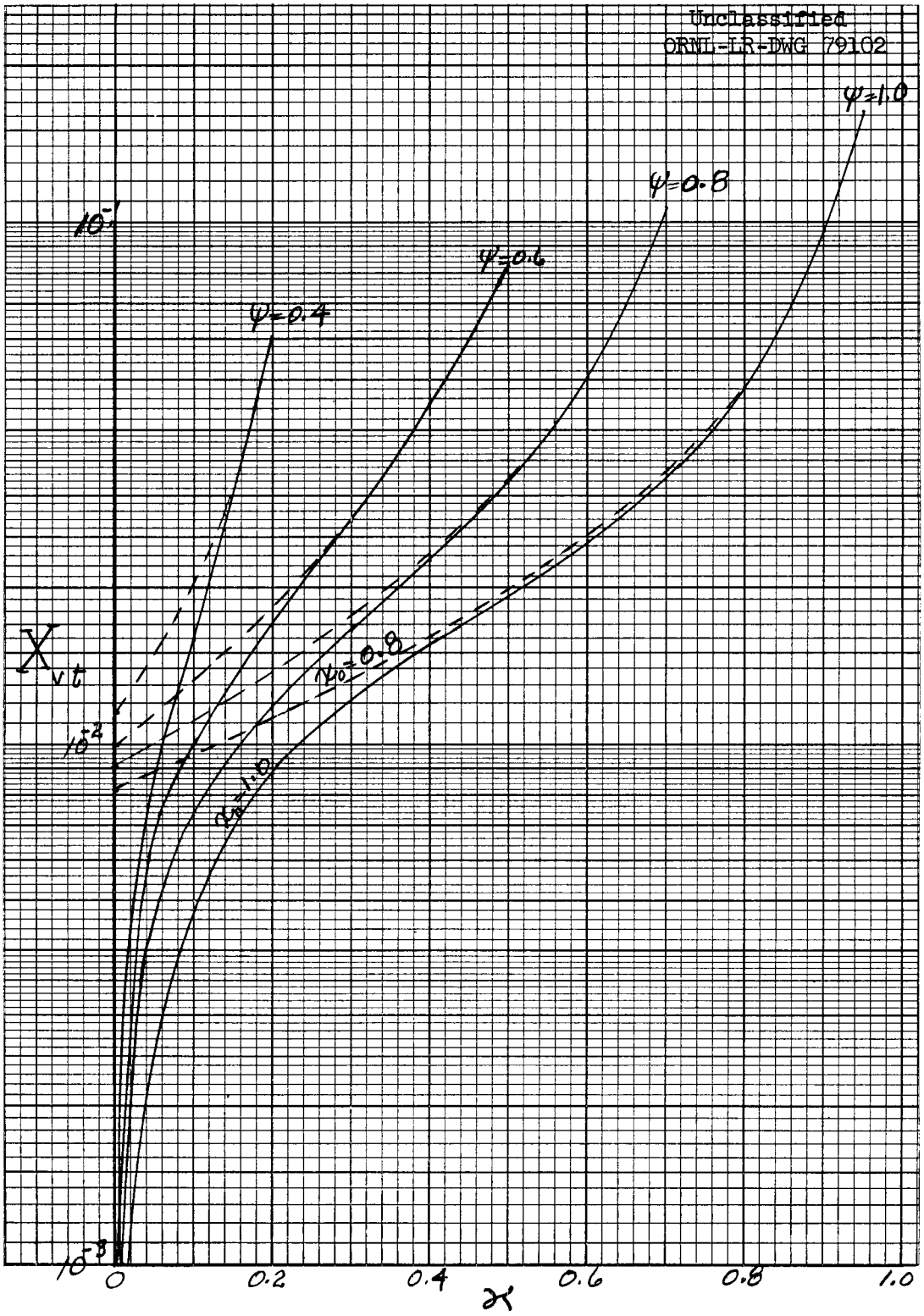

Fig. 17. Flow Modulus for Condensing Potassium at 1500°R in Tapered Tubes vs Tube Position, κ, Fraction Flow, ψ, and Entering Quality, x_o.

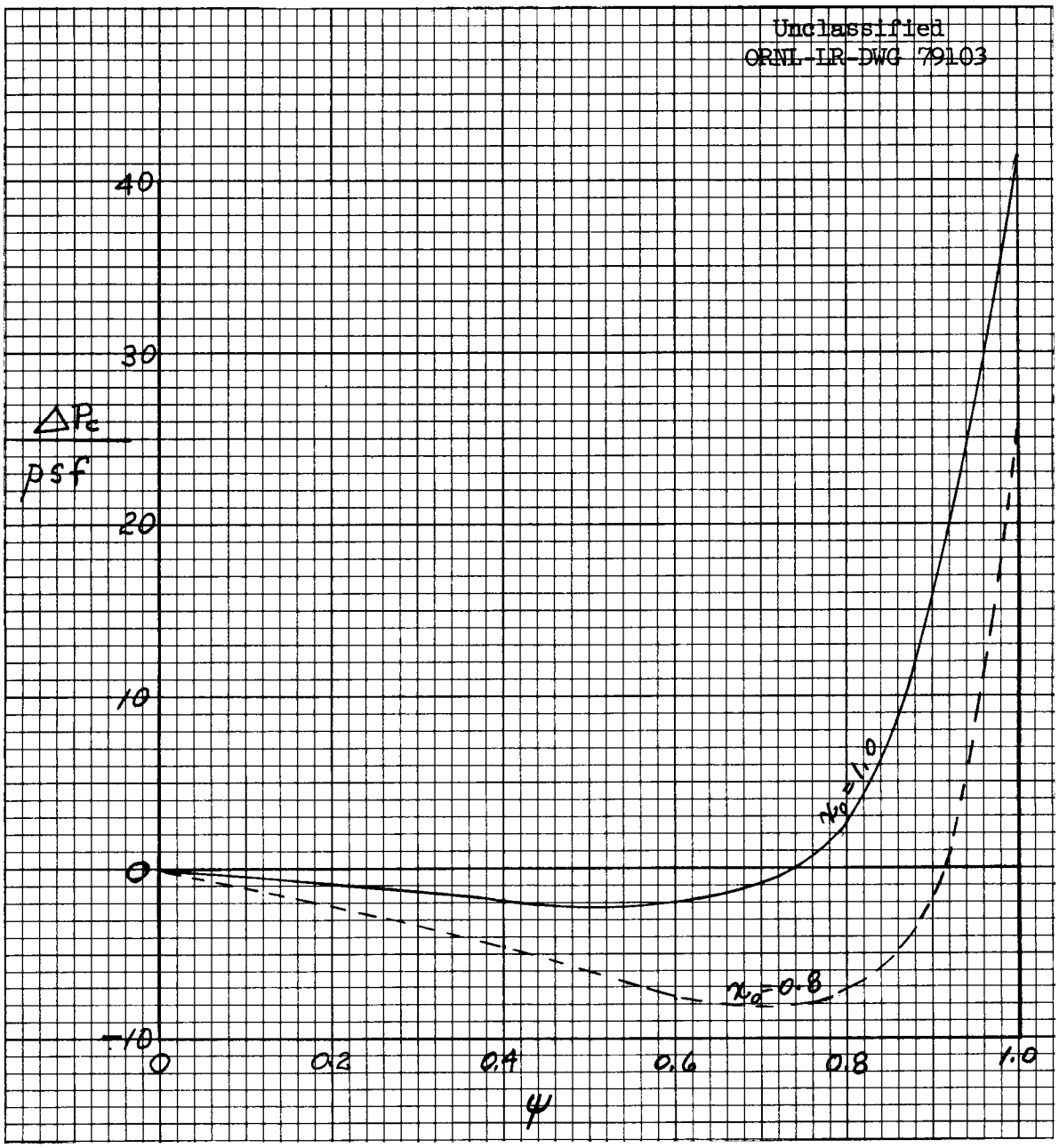

Fig. 18. Condensing Pressure Drop vs Inlet Vapor Flow for Condensing Potassium in Tapered Tubes at Constant Heat Flux, Case I.

between 62 and 66% of that at which the net drop is zero (the datum flow) for an inlet vapor quality of 1.0.[8] As may be estimated from Fig. 18, the corresponding minima for the Case I tapered tube are at about 70 to 75% of the datum flow, or 50 and 70% of design flow for inlet vapor qualities of 1.0 and 0.8 respectively. Also, for cylindrical tubes the momentum pressure recovery is 1.4 times the frictional pressure drop at the minimum, whereas the value applicable to Fig. 18 ($x_o = 1.0$) is 1.5. The difference is probably not significant. The corresponding ratio for the case where $x_o = 0.8$ is unrealistically high (3.0) because of the assumption that the entering liquid entrainment velocity equaled that of the vapor.

It is not possible to draw general comparisons quantitatively between condensing flow in cylindrical tubes and that in tapered tubes without having plotted curves such as Fig. 18 for a fairly wide variety of design conditions. However, it does appear that the pressure drop minima occur at higher relative flows in tapered tubes than in cylindrical ones for the same heat fluxes and condensing pressures.

In the curves of Fig. 18, the extremely steep slopes between $\psi = 0.8$ and 1.0 indicate extreme stability in this operating region because a small drop in flow brings about a steep pressure rise, tending to hold the flow steady. On the other hand, operation at ψ values less than about 0.7 could lead to instability. This unstable region can be reached, however, only by setting the operating point of the condenser at this value of ψ. As long as the condenser operating point exceeds a ψ value of 0.8 the condensate manifold pressure will always be lower than the inlet pressure, and back flow cannot occur, except perhaps momentarily during severe transients. For a properly designed space radiator-condenser, instability cannot occur from operation at fractional power because the condensing temperature must necessarily drop below the full-power value essentially as Stefan's law. Although the drop may be small the reduction in condensing pressure is large for liquid metals with the result that ρ_g drops rapidly and ΔP_{TP} rises accordingly. Thus, power changes slow enough to allow the heat flux to keep close to the steady-state value cannot bring about instability.

In conclusion, it appears that instability can be encountered only by operating the system with too low an effective L/D of the condenser tubes for the existing condensing conditions and working fluid.[9] This situation can in fact arise in only two ways in a Rankine space power system: (1) through the introduction of excess liquid inventory at reduced power, and (2) by the design of the radiator-condenser for insufficient ΔP_c at design power in the first place.

Table of Nomenclature

A	cross-sectional flow area, ft^2
A_h	heat transfer area, ft^2
D	tube inside diameter, ft
$\mathcal{D}$	tube outside diameter, ft
F	force due to momentum change, lbf
G	mass velocity, $lbm/hr \cdot ft^2$
H	latent heat of vaporization, Btu/lbm
K	Lockhart-Martinelli flow modulus coefficient
L	tube length, ft
M	Mach number
N_R	Reynolds number
P	pressure, lbf/ft^2
Q	heat flow, Btu/hr
T	temperature, °R
V	velocity, ft/hr
W	weight flow (design conditions), lbm/hr
w	reduced weight flow, lbm/hr
X	Lockhart-Martinelli flow modulus
b	fin thickness, ft
f	Fanning friction factor
g_c	mass-force conversion coefficient, 4.18×10^8 $lbm \cdot ft/lbf \cdot hr^2$
h	gas film heat transfer coefficient, $Btu/hr \cdot ft^2 \cdot °F$
h_e	equivalent heat transfer coefficient at radiating surface, $Btu/hr \cdot ft^2 \cdot °F$
k	thermal conductivity, $Btu/hr \cdot ft^2 \cdot °F/ft$
s	fin span, ft
v	velocity, ft/sec
x	vapor quality
y	fin height, ft
z	distance along tube from inlet, ft
σ	Stefan-Boltzmann constant, 0.171×10^{-8} $Btu/hr \cdot ft^2 \cdot T^4$
α	internal tube reduction ratio, $(D_o - D_L)/D_o$
β	external tube reduction ratio, $(\mathcal{D}_o - \mathcal{D}_L)/\mathcal{D}_o$
γ	view factor

ϵ	emissivity
ω	density reduction ratio, $(\rho_o - \rho_L)/\rho_o$
ξ	fin efficiency
κ	normalized tube length, z/L
ψ	normalized reduced inlet weight flow, w_{go}/W_{go}
ρ	density, lbm/ft^3
μ	viscosity, lbm/ft·hr
λ	condensation length, ft
ϕ	Lockhart-Martinelli two-phase flow modulus
η	fin efficiency ratio, $(\xi_o - \xi_L)/\xi_o$

Subscripts

o	inlet
h	heat transfer
z	variable, function of z
L	outlet
g	gas phase
ℓ	liquid phase
m	momentum
r	radiation
TP	two phase
c	condensing
v	viscous
t	turbulent
λ	function of λ
x	external

Notes

Physical Properties of Potassium at 1500°R

H	=	887 Btu/lbm
μ_v	=	0.0418 lbm/ft·hr
ρ_v	=	3.6×10^{-3} lbm/ft^3
ρ_ℓ	=	44 lbm/ft^3
μ_ℓ	=	0.399 lbm/ft·hr
P_{sat}	=	1.5 psia

Copper

Conductivity of copper 200 Btu/hr·ft^2·°F/ft

References

1. R. W. Lockhart and R. C. Martinelli, "Proposed Correlation of Data for Isothermal Two-Phase, Two-Component Flow in Pipes", Chem. Eng. Prog. 45: 39 (1949).

2. C. J. Baroczy and V. D. Sanders, "Pressure Drop for Flowing Vapors Condensing in a Straight Horizontal Tube", USAEC Report NAA-SR-6333, North American Aviation, June 1, 1961.

3. "Space Power Program Semiannual Progress Report for Period Ending December 31, 1961", USAEC Report ORNL-3270, Oak Ridge National Laboratory, April 26, 1962. (Classified)

4. K. A. Gardner, "Efficiency of Extended Surfaces", Trans. ASME, pp 621-7 (1945).

5. W. H. McAdams, Heat Transmission, McGraw-Hill Book Co., Inc., New York, 3rd ed., 1954, Fig. 6-11, p. 156.

6. G. J. Van Wylen, Thermodynamics, John Wiley & Sons, New York, 1959, pp 345-9.

7. H. R. Kunz, et al., "First Quarterly Report on Experimental Investigation of Heat Rejection Problems in Nuclear Space Power Plants, June 1 to August 31, 1962", USAEC Report PWA-2100, Pratt & Whitney Aircraft, pp 22-5.

8. Ibid., p. 66.

9. Ibid., p. 65.

Internal Distribution

1. S. E. Beall
2. M. Bender
3. A. L. Boch
4. R. B. Briggs
5. J. Foster
6-11. A. P. Fraas
12. A. G. Grindell
13. H. W. Hoffman
14. J. J. Keyes
15-20. R. B. Korsmeyer
21. M. E. LaVerne
22. R. N. Lyon
23. H. G. MacPherson
24. W. D. Manly
25. J. W. Michel
26. A. J. Miller
27. A. M. Perry
28. M. W. Rosenthal
29. H. W. Savage
30. A. W. Savolainen
31. M. J. Skinner
32. J. A. Swartout
33. D. B. Trauger
34. M. M. Yarosh
35-36. Central Research Library
37-39. Y-12 Document Reference Section
40-42. Laboratory Records Department
43. Laboratory Records — RC

External Distribution

44. C. H. Armbruster, Wright-Patterson Air Force Base, Dayton, Ohio
45. G. M. Anderson, AEC-Washington
46. J. W. Bjerkle, Sundstrand, Denver, Colorado
47. M. C. Coombs, Atomics International, Canoga Park, California
48. A. Koestel, Thompson Ramo-Wooldridge, Cleveland, Ohio
49. S. Lieblein, NASA Lewis Research Center, Cleveland, Ohio
50. R. M. Meyer, Pratt & Whitney, Hartford, Connecticut
51. K. Parker, AiResearch, Phoenix, Arizona
52. R. Schaupp, Aerojet-General Nucleonics, San Ramon, California
53. R. M. Scroggins, AEC-Washington
54. M. J. Whitman, AEC-Washington
55-69. Division of Technical Information Extension
70. Research and Development Division, ORO
71-72. Reactor Division, ORO